https://doi.org/10.5194/soil-2021-88
Preprint. Discussion started: 1 September 2021

The response of desert biocrust bacterial communities to hydration-desiccation cycles

Capucine Baubin*, Noya Ran, Hagar Siebner, Osnat Gillor*

Zuckerberg Institute for Water Research, Blaustein Institutes for Desert Research, Ben-Gurion University of the Negev, Midreshet Ben-Gurion, Israel

Correspondence to:

*Capucine Baubin, Zuckerberg Institute for Water Research, Blaustein Institutes for Desert Research, Ben-Gurion University of the Negev, Midreshet Ben-Gurion, Israel. Tel: 972-54-2944886; e-mail: baubin@post.bgu.ac.il

*Osnat Gillor, Zuckerberg Institute for Water Research, Blaustein Institutes for Desert Research, Ben-Gurion University of the Negev, Midreshet Ben-Gurion, Israel. Tel: 972-8-6596986; e-mail: gilloro@bgu.ac.il

https://doi.org/10.5194/soil-2021-88
Preprint. Discussion started: 1 September 2021

ABSTRACT

Rain events in arid environments are highly unpredictable, interspersing extended periods of drought. Therefore, tracking changes in desert soil bacterial communities during hydration-desiccation cycles in the field, was seldom attempted. Here, we assessed rain-mediated dynamics of active community in the Negev Desert biological soil crust (biocrust), and evaluated the changes in bacterial composition, potential function, photosynthetic activity, and extracellular polysaccharide (EPS) production. We predicted that increased biocrust moisture would resuscitate the phototrophs, while desiccation would inhibit their activity. Our results show that hydration increased chlorophyll content, resuscitated the biocrust *Cyanobacteria*, enhanced EPS production, and induced potential phototrophic functions. However, decrease in the soil water content did not immediately decrease the phototrophs activity, though chlorophyll levels decreased. Moreover, while the *Cyanobacteria* relative abundance significantly increased, *Actinobacteria*, the former dominant taxa, significantly decreased in abundance. We propose that, following a rain event, the response of the active bacterial community lagged the soil moisture content due to the production of EPS which delayed the desiccation of the biocrust community.

Key words: hydration; biocrust; bacteria; *Cyanobacteria*; *Actinobacteria*; EPS

https://doi.org/10.5194/soil-2021-88
Preprint. Discussion started: 1 September 2021

1. INTRODUCTION

Arid environments are the largest terrestrial biomes on Earth and accounts for 35% of the landmass (Pointing and Belnap, 2012). Rain in hot arid environments is rare and unpredictable, and the main source of water is dew (Malek et al., 1999), or fog (Kidron et al., 2002). This moisture is readily absorbed to the soil surface but would quickly evaporate due to high temperatures and low humidity (Cameron and Blank, 1966). The long droughts in drylands limit plant growth and in their stead, the soil is covered by microbial mats, named biological soil crust (biocrust). Biocrusts are a matrix of phototroph and heterotroph microorganisms that are bind together with soil particles, by using extracellular polymeric substances (Campbell et al., 1989; Belnap and Lange, 2001; Kidron et al., 2020). The biocrust phototrophs are the main primary producers in this desolate habitat and together with the heterotrophs, they form a rigid and stable mat that can resist to xerification and soil erosion (Bowker et al., 2018; Aanderud et al., 2019).

Biocrusts are the main source of carbon and nitrogen (Agarwal et al., 2014), and a strong contributor of soil respiration(Castillo-Monroy et al., 2011) in deserts. It was recently shown that, during long droughts many of the biocrust microorganisms rely not only on photosynthesis but also on oxidation of atmospheric trace gases(Meier et al., 2021; Leung et al., 2020). Once the biocrust is hydrated, the phototrophs respond quickly by inducing their photosynthetic systems and related functions, to take full advantage of the rare water abundance before the soil dehydrates (Murik et al., 2017). To that end, photosynthetic members of the biocrust community form a seed bank of species that can spring to life whenever the water content increases (Murik et al., 2017; Lennon and Jones, 2011; Kedem et al., 2020). Yet, the abrupt hydration may also cause osmotic shock that could result in massive cell lysis and the release of osmoregulatory solutes (Halverson et al., 2000; Harris, 1981). The period of water abundance is usually brief, and the soil quickly dehydrates forcing the bacteria to cease their activity (Murik et al., 2017; Oren et al., 2019). Therefore, the members of the biocrust community must respond quickly and efficiently not only to hydration but also to the subsequent desiccation.

https://doi.org/10.5194/soil-2021-88
Preprint. Discussion started: 1 September 2021

Earlier studies focused on community structure and cyanobacterial response to hydration-desiccation cycles under controlled conditions (Angel and Conrad, 2013; Wu et al., 2013; Meier et al., 2020; Oren et al., 2019). To the best of our knowledge, these cycles were never monitored in the field during a rain event. Under natural conditions, the biocrust community dynamics of the hydration-desiccation cycle may be affected by a plethora of variables, such as temperature, rain intensity, or soil local structure, which could not be applied in laboratory settings. Thus, it is imperative to elucidate the resuscitated community and its response to the gradual dehydration after a rain event in the field.

In this study, we followed the community structure and activity before, during, and after a rain event in the arid Negev Desert highlands (Israel). We studied the active biocrust community by using SSU ribosomes as a proxy to active bacterial community (Šťovíček et al., 2017). Although ribosomes do not quickly degrade in dormant or even dead cells (Sunyer-Figueres et al., 2018; Sukenik et al., 2012), under field conditions they present a reliable mean to distinguish between active and inactive cells (Šťovíček et al., 2017; Angel et al., 2013; Baubin et al., 2019). We hypothesised that the biocrust community would quickly respond to hydration and to desiccation. We predicted that high soil moisture would trigger photosynthetic activity and carbohydrate production and a decreasing soil moisture will lead to an inactivation of the phototrophs within the biocrust community. We further predicted that heterotrophs response to hydration-desiccation would differ among phyla as previously found for biocrust (Angel and Conrad, 2013) and topsoil (Šťovíček et al., 2017) collected from the same site. Specifically, we predicted a sharp decrease in the relative abundance of Actinobacteria phylum that dominants the soil during droughts but declines upon hydration (Šťovíček et al., 2017; Angel et al., 2013; Blazewicz et al., 2013).

https://doi.org/10.5194/soil-2021-88
Preprint. Discussion started: 1 September 2021

2. MATERIAL AND METHODS

2.1. Sampling

The study was conducted in the long-term ecological research station in the Negev Desert Highlands (Zin Plateau, 30°86'N, 34°80'E, Israel; Figure 1). In this arid environment, the average annual rainfall is around 90 mm and extends from October to April. Biocrust samples were collected on 20/06/17 during the dry season (T[0]; average temperature: 32.4°C) and during a rain event in the wet season from 29/01/18 through 01/02/18 at 24 hr intervals. The rain event (5.1 mm, maximum average temperature 14.6 °C) occurred 29/01/18 (T[R]) and samples were collected till the biocrust dried (T[1], T[2], T[3]; Figure 1) For each time point, five samples (each ~200 g) at least 10 m apart were collected (N = 25 samples). The biocrust samples were homogenised using a 2 mm sieve and then four subsamples were stored: (1) at -80°C for molecular analysis; (2) at -20°C for chlorophyll extraction; (3) at 60°C for 3 days and then kept at room temperature for chemical analysis; and (4) was used immediately to evaluate the water content.

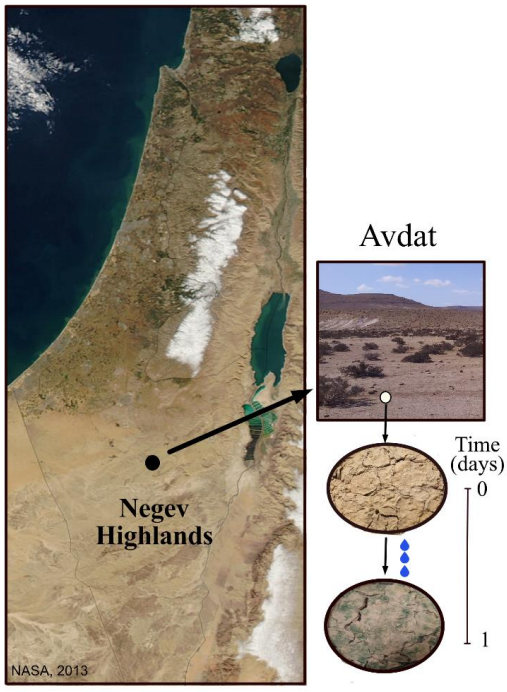

Figure 1. Location of the sampling site (Avdat) in the Negev Highlands (Israel) with close-ups of the crust at time 0 (before hydration) and at time 1 (after hydration). The crust becomes greener after a rain event.

https://doi.org/10.5194/soil-2021-88
Preprint. Discussion started: 1 September 2021

2.2. Physico-chemical analyses

Water content, organic carbon and total nitrogen were measured in the soil samples. Biocrust water content was determined by the gravimetric method, the soil was weighed before and after oven drying at 105ºC, then the percentage of moisture in the soil was determined (Scrimgeour, 2008). Organic carbon content was determined using the loss-on-ignition method. 30 g of the dry soil sample was burnt at 380°C for 6 hours, and the fraction of organic carbon content was calculated as previously described (Scrimgeour, 2008; Hoogsteen et al., 2015). Total nitrogen was measured in 50 mg of soil using the FlashSmart CHNS/O elemental analyser (ThermoFischer, Waltham, MA, USA). The standards: BBOT (2,5-Bis (5-tert-butyl-benzoxazol-2-yl) thiophene), Tocopherol Nicotinate and a soil reference material were used to calibrate the instrument.

2.3. Chlorophyll concentration and water content

The chlorophyll of each sample was extracted using a protocol based on Ritchie (2006) and Castle et al. (2010). The extraction was done using methanol, with a soil: methanol ratio of 3:9, followed by a 15-minutes incubation at 65°C and a 2-hour incubation at 4°C. The samples were centrifuged, and the supernatant was measured by spectrophotometry (Infinite 200 Pro, Tecan, Switzerland) at 665 nm and the concentration of chlorophyll was calculated following (Ritchie, 2006). Dried Spirulina cultures were used as positive control at 0.003g per g of soil. Distilled water (DW) was used as negative controls. The concentrations are presented in mg chlorophyll per g of soil (mg chla/g soil).

2.4. Carbohydrate extraction and Polysaccharide content

Extracellular polysaccharides (EPS), and more precisely the tightly-bound carbohydrates that are attached to the soil particles, were extracted using a 100 mM EDTA solution for 16 hours. About 20 mL of EPS were extracted from 2.5 g of soil and were kept at -20°C until further processing. The polysaccharide content was measured using a phenol-sulfuric acid assay with a glucose standard curve, as previously described (Dubois et al., 1956). Briefly, each EPS fraction was combined with equal volume of 5% w/v phenol and 2.5 folds sulfuric acid. The mixture was vortexed, incubated

https://doi.org/10.5194/soil-2021-88
Preprint. Discussion started: 1 September 2021

(45 min at room temperature) and absorbance measured at 490 nm (Infinite 200 Pro, Tecan, Switzerland).

2.5. RNA extraction and preparation for sequencing

RNA was extracted from 0.5 – 1 g of soil using phenol-chloroform, following a previously described protocol (Angel, 2012). The extracted total nucleic acids were treated with DNase (Takara, Shiga, Japan) to remove the DNA. The remaining RNA was cleaned using the *MagListo* RNA Extraction kit (Bioneer, Daejeon, South Korea). The RNA was reverse transcribed to cDNA using Superscript IV (ThermoFischer, Waltham, MA, USA), and purified using the PCR purification kit (Bioneer, Daejeon, South Korea) in accordance with the manufacturers' instructions. The cDNA was used as a template to amplify the V3-V4 regions of the 16S rRNA using 341F and 806R primers (Table A1), in triplicates. Library preparations and sequencing were performed at the Research Resource Centre at the University of Illinois with pair end (2 × 300 bp) MiSeq platform (Illumina, San Diego, CA, USA). Due to low concentrations of ribosomes in the dry soil collected during the summer of 2017, we had to re-extract and re-sequence these samples. However, COVID-19 restrictions prohibit us from using the same sequencing platform, and we were forced to use the facilities and resources available to us at the time. Therefore, RNA was extracted using the RNeasy PowerSoil Total RNA Kit (Qiagen, Hilden, Germany), following the manufacturer's protocol. Then, the V3-V4 regions of the 16S rRNA were amplified using 341F and 515R primers (Table A1), in triplicates. The samples were sequenced (2 × 150 bp) on the iSeq platform (Illumina, San Diego, CA, USA) at the Central and Northern Arava R&D Centre (Israel).

2.6. Community analysis

Reads were merged, quality checked, and trimmed following the NeatSeq-Flow pipeline (Sklarz et al., 2018). The sequences were analysed using QIIME2 (Bolyen et al., 2018) and Dada2 (Callahan et al., 2016). Reads were clustered in amplicon sequence variants (ASVs) and taxonomy was assigned using Silva v138 (Quast et al., 2013). The total number of sequences can be found in Table A2. All raw sequences used in this study can be found in BioProject (https://www.ncbi.nlm.nih.gov/ bioproject) under the submission number PRJNA718159.

https://doi.org/10.5194/soil-2021-88
Preprint. Discussion started: 1 September 2021

2.7. Functional predictions

Functional predictions of the 16S amplicons were done using Piphillin (Narayan et al., 2020; Iwai et al., 2016) and the KEGG database with a 97%-identity cut-off (May 2020) (Kaneshisa and Goto, 2000). Steps of metabolic pathways for different methods of harvesting energy (organotrophy, lithotrophy and phototrophy) (Cordero et al., 2019; Greening et al., 2016; León-Sobrino et al., 2019; Tveit et al., 2019), for parts of the nitrogen cycle (Galloway et al., 2004), and for the survival of the individual during a drought (DNA conservation and repair, sporulation and Reactive Oxygen Species (ROS)-damage prevention) (Borisov et al., 2013; Hansen et al., 2007; Henrikus et al., 2018; Preiss, 1984; Preiss and Sivak, 1999; Rajeev et al., 2013; Repar et al., 2012; Slade and Radman, 2011)were selected. Then, we picked out genes of interest from each step in the KEGG database and built our own database (Table A3). The assignment of function to the KEGG numbers of the abundance table from Piphillin was done in R using phyloseq (McMurdie et al., 2017). The significance of temporal differences in predicted functionalities was evaluated using a non-parametric test (Kruskal-Wallis test and a post-hoc Dunn test (Dinno, 2017; Dunn, 1964; Kruskal and Wallis, 1952).

2.8. Statistical analysis

All statistical analysis was done using R (R: A language and environment for statistical computing) using the phyloseq (McMurdie et al., 2017) along with the ggplot2 (Wickham, 2016), vegan (Oksanen et al., 2014), magritt (Wickham and Bache, 2014), dplyr (Wickham et al., 2018), scales (Wickham, 2017), grid (Murrell, 2004) packages. The significance of difference between time points was determined using a non-parametric test: Kruskal-Wallis test and Dunn test (Dinno, 2017; Dunn, 1964; Kruskal and Wallis, 1952).

https://doi.org/10.5194/soil-2021-88
Preprint. Discussion started: 1 September 2021

3. RESULTS

3.1. Temporal changes in the biocrust chlorophyll, carbohydrates, and chemical analyses

We have followed changes in the biocrust before, during and after a rain event and noted that a day after the rain (T[1]) the biocrust in the sampling site was visibly greener than at any other sampling point (Figure 1). The average chlorophyll concentrations along with the soil water content in the biocrust at each sampling point were monitored (Figure 2A, Table A4). The biocrust water content was lower at the dry season T[0] and significantly increased during the rain event T[R] (2.26% and 16.2%, respectively, $p = 0.05$; Table A5). Then soil moisture significantly decreased to 3.67% at T[3] ($p < 0.05$). The chlorophyll concentrations significantly increased right after the rain event (from 8.45 mg chla/g soil to 14.57 mg chla/g soil, during the rain event, $p = 0.0002$; Table A4 and A5), but decreased significantly in later days (from 14.57 mg chla/g to 11.17 mg chla/g soil, three days after the rain, $p > 0.02$; Table A4 and A5). However, the carbohydrate concentration significantly increases after the rain event (from 83 µg/g soil to 143 µg/g soil, $p < 0.05$, Table A4 and A5, Figure 2B). After the first day, the concentration decreased slowly until day 3, where it was significantly lower (from 143 µg/g soil to 72 µg/g soil, $p < 0.05$, Table A4 and A5, Figure 2B). The total organic carbon (Figure B1) and total nitrogen (Figure B2) showed slight temporal changes (Table A4) that were not significant (Table A5).

https://doi.org/10.5194/soil-2021-88
Preprint. Discussion started: 1 September 2021

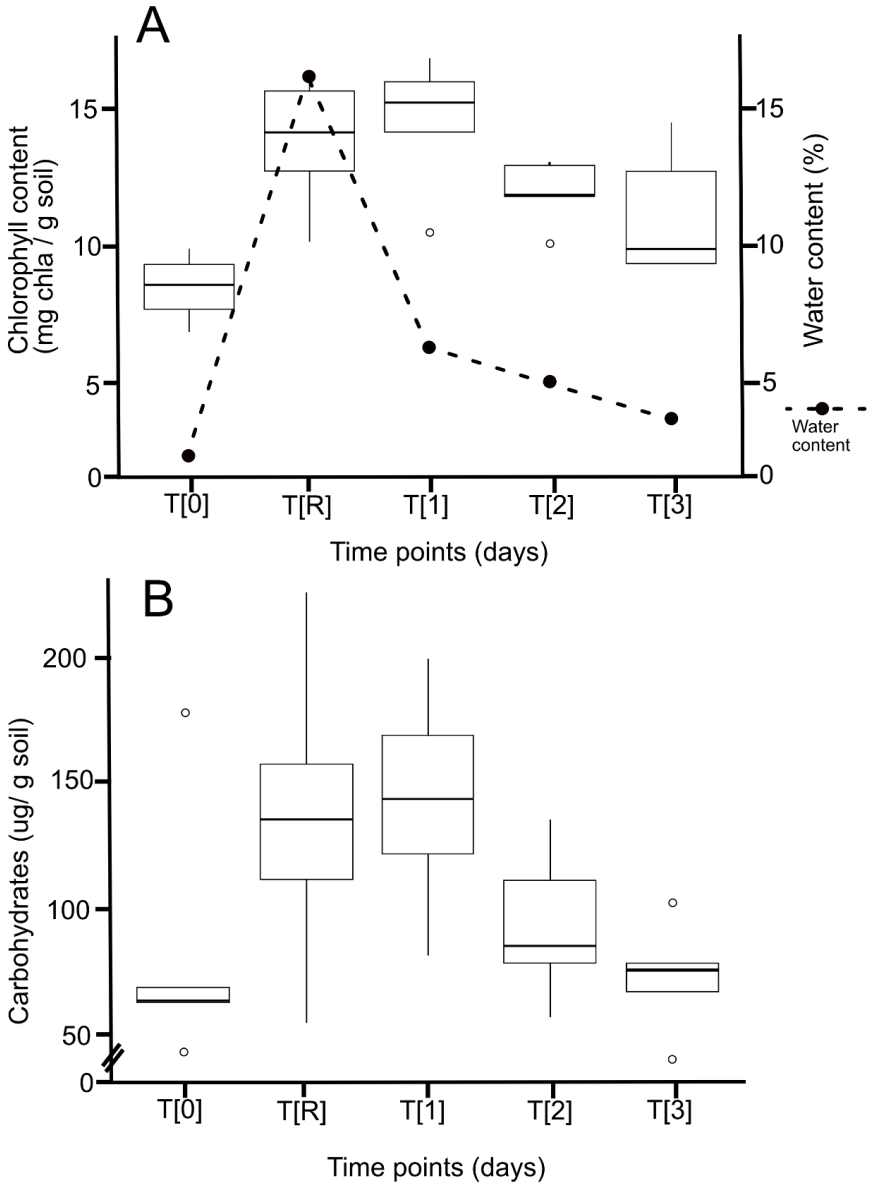

Figure 2A. Chlorophyll content (in mg chla/g soil) (boxplot) and water content (in %) (line and points) for each time point. Both increase at T[R] and decrease rapidly after.

Figure 2B. Carbohydrate concentration (in µg/g soil) (boxplot) for each time point. The concentration increases rapidly after the rain event and decreases slowly until T[3].

https://doi.org/10.5194/soil-2021-88
Preprint. Discussion started: 1 September 2021

3.2. Temporal changes in the microbial community composition

Figure 3 shows the bacterial community composition at the order level for each sampling point. The community is mostly composed of the phyla *Cyanobacteria*, *Actinobacteria*, and *Proteobacteria* (Figure 3; Table A6). During the dry season, biocrust community composition differed significantly from the community depicted during the rain event (Table A7). The differences were shown mostly in orders belonging to the *Actinobacteria* and *Cyanobacteria* phyla (Figure 3; $p < 0.05$, Table A7). The relative abundance of *Cyanobacteria*, dominated by the *Cyanobacteriales*, increased during the rain event (from 22% to 41%, Table A6; $p < 0.05$, Table A7). While the relative abundance of the *Actinobacteria*, dominated by *Micrococcales*, decreased during the rain event (from 50% to 19%, Table A6; $p < 0.05$, Table A7). In the days following the rain event, no major changes were detected in the biocrust community (Figure 3; Table A6 and A7).

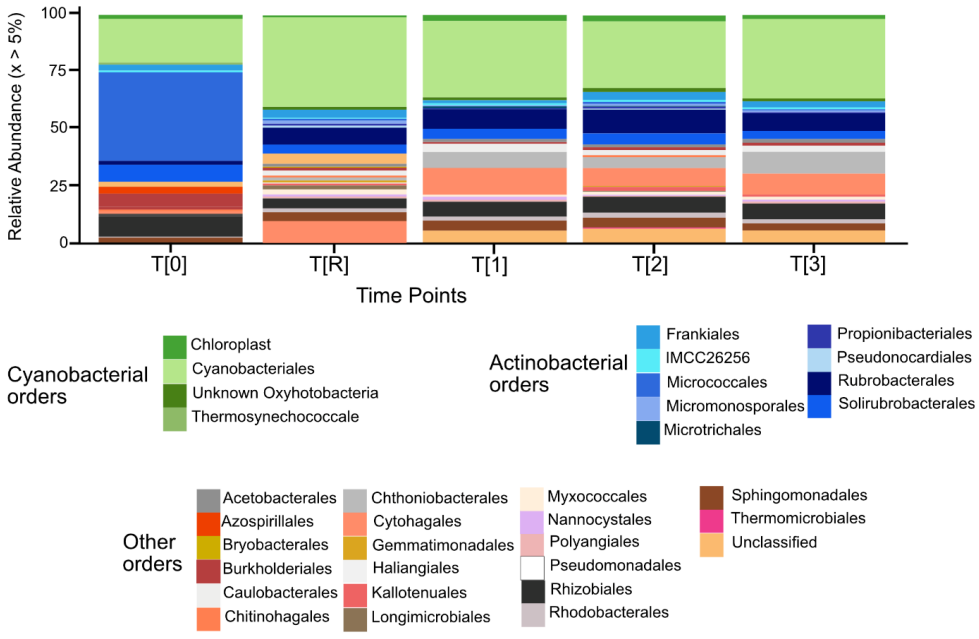

Figure 3. Relative abundance (in %, x> 0.05) at the order level for each time point. The cyanobacterial orders are gathered and in different shades of green, the actinobacterial orders are gathered and in different shades of blue, and the rest of the orders are gathered alphabetically. The abundance of

https://doi.org/10.5194/soil-2021-88
Preprint. Discussion started: 1 September 2021

Cyanobacterial orders decreases at T[R], while the abundance of the Actinobacterial orders increases at T[R].

3.3. Temporal changes in the microbial function

Figure 4 shows the predicted function based on the taxonomic composition using Piphillin displayed in copy number (CN). The values were significantly lower ($p < 0.03$; Table A9) in the dry season compared to the hydration-desiccation cycle, except for light and energy sensing (Figure 4; Table A8).

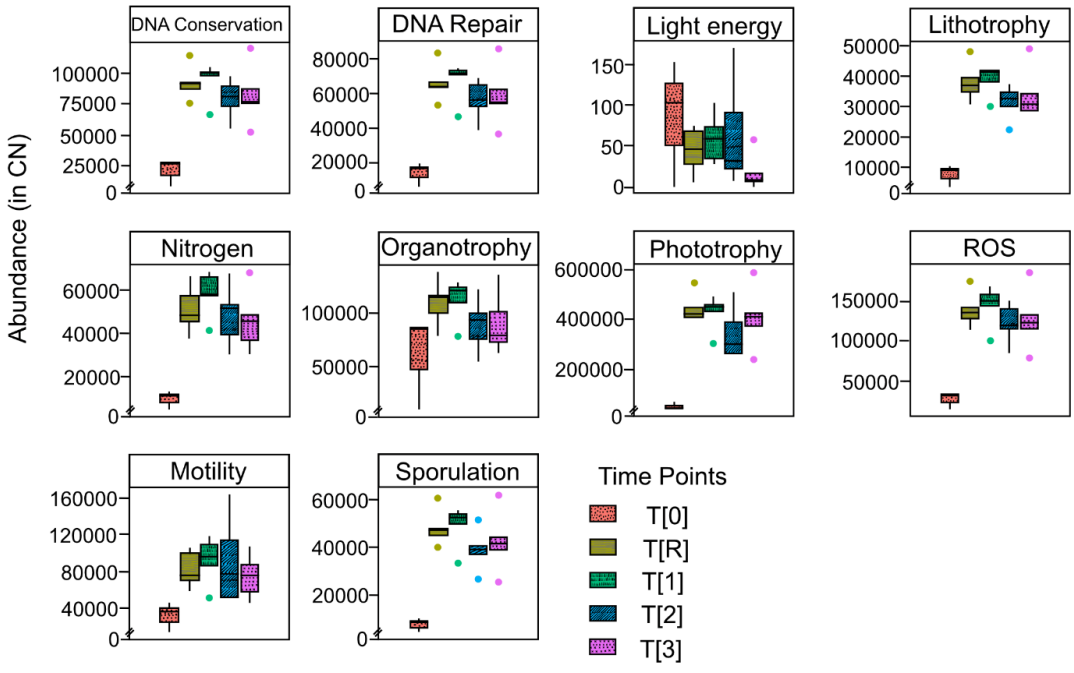

Figure 4. Boxplots of the functional prediction of the 16S sequences. Each panel (Boxplot) represents a different group of genes associated with a certain functionality. The full list of genes can be found in Table A3. The time points are represented by distinct colours and patterns. The y-axis is the abundance in copy number (CN) normalized to the 16S rRNA copy number for each genome.

https://doi.org/10.5194/soil-2021-88
Preprint. Discussion started: 1 September 2021

4. DISCUSSION

Biocrust bacterial communities were shown to alter during hydration (Angel and Conrad, 2013; Meier et al., 2021). Most apparent was the change in the relative abundance of Cyanobacteria which increased while the abundance of Actinobacteria decreased (Figure 3), similar to results obtained under controlled conditions where the biocrust was hydrated to saturation (Angel and Conrad, 2013). Likewise, the filamentous cyanobacterium Leptolyngbya sp. isolated from the Negev Desert biocrust, was shown to respond quickly to both hydration and desiccation (Oren et al., 2019, 2017). Even slight increases in biocrust moisture, triggered by dew simulation, were shown to induce DNA repair and associated regulatory genes, activating the photosynthetic system of the cyanobacterium (Rajeev et al., 2013; Murik et al., 2017). In the field, a rain event significantly increases soil moisture (Figure 2A), activating various cyanobacterial orders (Figure 3) that trigger their photosynthesis system (Figure 4), resulting in a sharp rise in bacterial chlorophyll a (Figure 2A) and carbohydrates (Figure 2B) concentrations. The concentration of the chlorophyll pigment was suggested to be linked to the soil water content (Péli et al., 2011) and to the activity of the biocrust primary producers, i.e., Cyanobacteria and/or green algae.

While the cyanobacterial activity increased with soil moisture (Figure 2A), no significant changes were detected in the total organic carbon and nitrogen content (Figure B1 and B2; Table A4 and A5). This observation suggests that the immediate change in these parameters is negligible compared to existing soil reservoir; thus, it cannot be used as an indicator for the resuscitation of the local microbial community during rain events. Moreover, it was recently proposed that in arid biocrusts, the dominant Cyanobacteria phylum exchanges carbon for nitrogen with copiotrophic diazotrophs, thus rapidly utilizing available nutrients to enable their colonisation of the oligotrophic dryland soils (Couradeau et al., 2019).

In arid soils, rain events entail a decrease in the abundance of Actinobacteria both in the biocrust (Angel and Conrad, 2013) and topsoil (Šťovíček et al., 2017; Barnard et al., 2013). Members of this phylum were shown to be well adapted to harsh environments (Goodfellow and Williams, 1983;

https://doi.org/10.5194/soil-2021-88
Preprint. Discussion started: 1 September 2021

Zvyagintsev et al., 2007), and were found to be abundant in the Negev Highland biocrust (Meier et al., 2021). Here, we showed that the increase of water content may lead to an increase in activity in all gene groups linked to energy usage or production (Figure 4; Table A9). The generally dry biocrust, experiences a narrow window of hydration conditions after a rain event (Figure 2A) that needs to be rapidly exploited by the primary producers before the soil dries (Figure 2A and 2B). Concomitantly, the resilient heterotrophs are mitigated, as was previously shown in controlled (Cordero et al., 2019; Greening et al., 2016; León-Sobrino et al., 2019; Tveit et al., 2019), and natural settings (León-Sobrino et al., 2019).

The microbial community quickly responds to hydration (Figure 3). However, the response to desiccation is slower despite the rapid drying of the biocrust (Figure 2A) due to evaporation, expedited by strong radiation, high winds, and low air humidity (Kidron and Tal, 2012). Unlike the response to dew hydration-desiccation cycles (Oren et al., 2019, 2017), the community does not immediately inactivate, when the water content in the soil decreases. In a previous study (Šťovíček et al., 2017), we showed that the topsoil community bounces back to its original structure as the soil dries. In the biocrust, while dehydration was associated to a decrease in chlorophyll concentrations (Figure 2A), there was no significant changes in the community composition (Figure 3). The concentration of carbohydrates, the main components of EPS, follows the same pattern as chlorophyll. In controlled experiments, it was shown that Cyanobacteria secrete copious amounts of EPS that bind the soil particles (Kidron and Tal, 2012; Kidron et al., 2020) and retain water in the soil, slowing down the drying process (Roberson and Firestone, 1992). EPS in the soil also create microhabitats that retain humidity (Colica et al., 2014), thus protecting the residing microorganisms from desiccation (Mazor et al., 1996; Mager and Thomas, 2011). In the Negev desert, a similar impact of the EPS production can be seen. Indeed, it may benefit soil microbial community by creating microhabitats in which moisture is retained longer, enabling an extended active phase following a rain event. This extra active time after a rain event enables longer photosynthesis. This provides access to organic molecules that may justify the ample resources invested by the Cyanobacteria in EPS production (Mager and Thomas, 2011). EPS was known as a key component in the Negev Desert for maintaining the structural

https://doi.org/10.5194/soil-2021-88
Preprint. Discussion started: 1 September 2021

integrity of the biocrust (Kidron et al., 2020) but it seems to help also sustaining the activity of the soil bacterial communities that inhabit the biocrust.

5. CONCLUSIONS

In desert biocrusts, bacterial communities must respond quickly and efficiently to hydration, to take advantage of this short window of opportunity and sequester nutrients. This fleeting abundance requires the bacterial community to be equally adapt to the onset of desiccation and prevent cells damage. Our findings reinforce controlled studies showing that biocrust hydration change the bacterial community and increasing cyanobacterial relative abundance over *Actinobacteria*. Here, we have shown that the response to biocrust desiccation following a rain event is slower than after a dew event, allowing the primary producers to be active even after the soil moisture decreases. This lag in response to dehydration could be associated to water retention by the newly secreted EPS, mediated by the *Cyanobacteria* activity surge. This grace period may justify the metabolic cost of polysaccharides exhaustive production that quickly follows rain events in the desert.

https://doi.org/10.5194/soil-2021-88
Preprint. Discussion started: 1 September 2021

ACKNOWLEDGEMENTS

The authors are grateful to Lusine Ghazaryan for technical support and to Ben Poodiack for editing the manuscript. This study was partially supported by the Israel Science Academy, grant no. 993/11.

DATA AVAILABILITY

The data (raw reads) are available in Bioproject under the submission number PRJNA718159.

COMPETING INTERESTS

The authors declare that they have no conflict of interest.

AUTHORS CONTRIBUTIONS

CB, OG and HS conceptualized and designed the methodology; CB and OG collected the samples and metadata; CB and NR did the laboratory work and sequencing; CB did the formal analysis, visualization, data curation and wrote the manuscript; CB, OG, HS and NR did the reviewing and editing of the manuscript.

https://doi.org/10.5194/soil-2021-88
Preprint. Discussion started: 1 September 2021

REFERENCES

Aanderud, Z. T., Bahr, J., Robinson, D. M., Belnap, J., Campbell, T. P., Gill, R. A., McMillian, B., and st. Clair, S.: The Burning of Biocrusts Facilitates the Emergence of a Bare Soil Community of Poorly-Connected Chemoheterotrophic Bacteria With Depressed Ecosystem Services, 7, 1–14, https://doi.org/10.3389/fevo.2019.00467, 2019.

Agarwal, L., Qureshi, A., Kalia, V. C., Kapley, A., Purohit, H. J., and Singh, R. N.: Arid ecosystem: Future option for carbon sinks using microbial community intelligence, 106, 1357–1363, 2014.

Angel, R.: Total Nucleic Acid Extraction from Soil, 2012.

Angel, R. and Conrad, R.: Elucidating the microbial resuscitation cascade in biological soil crusts following a simulated rain event, 15, 2799–2815, https://doi.org/10.1111/1462-2920.12140, 2013.

Angel, R., Pasternak, Z., Soares, M. I. M., Conrad, R., and Gillor, O.: Active and total prokaryotic communities in dryland soils, 86, 130–138, https://doi.org/10.1111/1574-6941.12155, 2013.

Barnard, R. L., Osborne, C. A., and Firestone, M. K.: Responses of soil bacterial and fungal communities to extreme desiccation and rewetting, 7, 2229–2241, https://doi.org/10.1038/ismej.2013.104, 2013.

Baubin, C., Farrell, A. M., Šťovíček, A., Ghazaryan, L., Giladi, I., and Gillor, O.: Seasonal and spatial variability in total and active bacterial communities from desert soil, 74, 7–14, https://doi.org/10.1016/J.PEDOBI.2019.02.001, 2019.

Belnap, J. and Lange, O. L.: Biological Soil Crusts: Structure, Function, and Management, 496 pp., https://doi.org/10.1639/0007-2745(2002)105[0500:]2.0.co;2, 2001.

Blazewicz, S. J., Barnard, R. L., Daly, R. A., and Firestone, M. K.: Evaluating rRNA as an indicator of microbial activity in environmental communities: Limitations and uses, 7, 2061–2068, https://doi.org/10.1038/ismej.2013.102, 2013.

Bolyen, E., Rideout, J. R., Dillon, M. R., Bokulich, N. A., Abnet, C., Al-Ghalith, G. A., Alexander, H., Alm, E. J., Arumugam, M., Asnicar, F., Bai, Y., Bisanz, J. E., Bittinger, K., Brejnrod, A., Brislawn, C. J., Brown, C. T., Callahan, B. J., Caraballo-Rodríguez, A. M., Chase, J., Cope, E., da Silva, R., Dorrestein, P. C., Douglas, G. M., Durall, D. M., Duvallet, C., Edwardson, C. F., Ernst, M., Estaki, M., Fouquier, J., Gauglitz, J. M., Gibson, D. L., Gonzalez, A., Gorlick, K., Guo, J., Hillmann, B., Holmes, S., Holste, H., Huttenhower, C., Huttley, G., Janssen, S., Jarmusch, A. K., Jiang, L., Kaehler, B., Kang, K. bin, Keefe, C. R., Keim, P., Kelley, S. T., Knights, D., Koester, I., Kosciolek, T., Kreps, J., Langille, M. G. I., Lee, J., Ley, R., Liu, Y.-X., Loftfield, E., Lozupone, C., Maher, M., Marotz, C., Martin, B. D., McDonald, D., McIver, L. J., Melnik, A. v, Metcalf, J. L., Morgan, S. C., Morton, J., Naimey, A. T., Navas-Molina, J. A., Nothias, L. F., Orchanian, S. B., Pearson, T., Peoples, S. L., Petras, D., Preuss, M. L., Pruesse, E., Rasmussen, L. B., Rivers, A., Robeson Michael S, I. I., Rosenthal, P., Segata, N., Shaffer, M., Shiffer, A., Sinha, R., Song, S. J., Spear, J. R., Swafford, A. D., Thompson, L. R., Torres, P. J., Trinh, P., Tripathi, A., Turnbaugh, P. J., Ul-Hasan, S., van der Hooft, J. J. J., Vargas, F., Vázquez-Baeza, Y., Vogtmann, E., von Hippel, M., Walters, W., Wan, Y., et al.: QIIME 2: Reproducible, interactive, scalable, and extensible microbiome data science, 6, e27295v2, https://doi.org/10.7287/peerj.preprints.27295v2, 2018.

Borisov, V. B., Forte, E., Davletshin, A., Mastronicola, D., Sarti, P., and Giuffrè, A.: Cytochrome bd oxidase from Escherichia coli displays high catalase activity: An additional defense against oxidative stress, 587, 2214–2218, https://doi.org/10.1016/j.febslet.2013.05.047, 2013.

Bowker, M. A., Reed, S. C., Maestre, F. T., and Eldridge, D. J.: Biocrusts: the living skin of the earth, 429, 1–7, https://doi.org/10.1007/s11104-018-3735-1, 2018.

Callahan, B. J., McMurdie, P. J., Rosen, M. J., Han, A. W., Johnson, A. J. A., and Holmes, S. P.: DADA2: High-resolution sample inference from Illumina amplicon data, 13, 581–583, https://doi.org/10.1038/nmeth.3869, 2016.

Cameron, R. E. and Blank, G. B.: Desert algae: soil crusts and diaphanous substrata as algal habitats, 47 pp., 1966.

Campbell, S. E., Seeler, J., and Golubic, S.: Desert crust formation and soil stabilization, 3, 217–228, https://doi.org/10.1080/15324988909381200, 1989.

Castillo-Monroy, A. P., Maestre, F. T., Rey, A., Soliveres, S., and Garcia-Palacios, P.: Biological Soil Crust Microsites Are the Main Contributor to Soil Respiration in a Semiarid Ecosystem, 14, 835–847, https://doi.org/10.1007/s10021-011-9449-3, 2011.

Castle, S. C., Morrison, C. D., and Barger, N. N.: Extraction of chlorophyll a from biological soil crusts: A comparison of solvents for spectrophotometric determination, 43, 853–856, https://doi.org/10.1016/j.soilbio.2010.11.025, 2010.

Colica, G., Li, H., Rossi, F., Li, D., Liu, Y., and de Philippis, R.: Microbial secreted exopolysaccharides affect the hydrological behavior of induced biological soil crusts in desert sandy soils, 68, 62–70, https://doi.org/10.1016/j.soilbio.2013.09.017, 2014.

Cordero, P. R. F., Bayly, K., Man Leung, P., Huang, C., Islam, Z. F., Schittenhelm, R. B., King, G. M., and Greening, C.: Atmospheric carbon monoxide oxidation is a widespread mechanism supporting microbial survival, 13, 2868–2881, https://doi.org/10.1038/s41396-019-0479-8, 2019.

Couradeau, E., Giraldo-Silva, A., de Martini, F., and Garcia-Pichel, F.: Spatial segregation of the biological soil crust microbiome around its foundational cyanobacterium, Microcoleus vaginatus, and the formation of a nitrogen-fixing cyanosphere, 7, 1–12, https://doi.org/10.1186/s40168-019-0661-2, 2019.

Dinno, A.: Package ‘dunn.test,’ 1–7, 2017.

Dubois, M., Gilles, K. A., Hamilton, J. K., Rebers, P. A., and Smith, F.: Colorimetric Method for Determination of Sugars and Related Substances, 350–356 pp., 1956.

Dunn, O. J.: Multiple Comparisons Using Rank Sums, 6, 241–252, 1964.

Galloway, J. N., Dentener, F. J., Capone, D. G., Boyer, E. W., Howarth, R. W., Seitzinger, S. P., Asner, G. P., Cleveland, C. C., Green, P. A., Holland, E. A., Karl, D. M., Michaels, A. F., Porter, J. H., Townsend, A. R., and Vörösmarty, C. J.: Nitrogen cycles: past, present, and future, 70, 153–226, 2004.

Goodfellow, M. and Williams, S. T.: Ecology of actinomycetes., 37, 189–216, https://doi.org/10.1146/annurev.mi.37.100183.001201, 1983.

Greening, C., Biswas, A., Carere, C. R., Jackson, C. J., Taylor, M. C., Stott, M. B., Cook, G. M., and Morales, S. E.: Genomic and metagenomic surveys of hydrogenase distribution indicate H 2 is a widely utilised energy source for microbial growth and survival, 10, 761–777, https://doi.org/10.1038/ismej.2015.153, 2016.

Halverson, L. J., Jones, T. M., and Firestone, M. K.: Release of Intracellular Solutes by Four Soil Bacteria Exposed to Dilution Stress, 64, 1630–1637, https://doi.org/10.2136/sssaj2000.6451630x, 2000.

Hansen, B. B., Henriksen, S., Aanes, R., and Sæther, B. E.: Ungulate impact on vegetation in a two-level trophic system, 30, 549–558, https://doi.org/10.1007/s00300-006-0212-8, 2007.

Harris, R. F.: Effect of Water Potential on Microbial Growth and Activity, https://doi.org/https://doi.org/10.2136/sssaspecpub9.c2, 1 January 1981.

Henrikus, S. S., Wood, E. A., McDonald, J. P., Cox, M. M., Woodgate, R., Goodman, M. F., van Oijen, A. M., and Robinson, A.: DNA polymerase IV primarily operates outside of DNA replication forks in Escherichia coli, 14, 1–29, https://doi.org/10.1371/journal.pgen.1007161, 2018.

Hoogsteen, M. J. J., Lantinga, E. A., Bakker, E. J., Groot, J. C. J., and Tittonell, P. A.: Estimating soil organic carbon through loss on ignition: Effects of ignition conditions and structural water loss, 66, 320–328, https://doi.org/10.1111/ejss.12224, 2015.

Iwai, S., Weinmaier, T., Schmidt, B. L., Albertson, D. G., Poloso, N. J., Dabbagh, K., and DeSantis, T. Z.: Piphillin: Improved prediction of metagenomic content by direct inference from human microbiomes, 11, 1–18, https://doi.org/10.1371/journal.pone.0166104, 2016.

Kaneshisa, M. and Goto, S.: KEGG: Kyoto Encyclopedia of Genes and Genomes, 28, 27–30, https://doi.org/10.3892/ol.2020.11439, 2000.

Kedem, I., Treves, H., Noble, G., Hagemann, M., Murik, O., Raanan, H., Oren, N., Giordano, M., and Kaplan, A.: Keep your friends close and your competitors closer: novel interspecies interaction in desert biological sand crusts, 00, 1–8, https://doi.org/10.1080/00318884.2020.1843349, 2020.

Kidron, G. J. and Tal, S. Y.: The effect of biocrusts on evaporation from sand dunes in the Negev Desert, 179–180, 104–112, https://doi.org/10.1016/j.geoderma.2012.02.021, 2012.

Kidron, G. J., Herrnstadt, I., and Barzilay, E.: The role of dew as a moisture source for sand microbiotic crusts in the Negev Desert, Israel, 52, 517–533, https://doi.org/10.1006/jare.2002.1014, 2002.

Kidron, G. J., Wang, Y., and Herzberg, M.: Exopolysaccharides may increase biocrust rigidity and induce runoff generation, 588, 125081, https://doi.org/10.1016/j.jhydrol.2020.125081, 2020.

Klindworth, A., Pruesse, E., Schweer, T., Peplies, J., Quast, C., Horn, M., and Glöckner, F. O.: Evaluation of general 16S ribosomal RNA gene PCR primers for classical and next-generation sequencing-based diversity studies, 41, 1–11, https://doi.org/10.1093/nar/gks808, 2013.

Kruskal, W. H. and Wallis, W. A.: Use of Ranks in One-Criterion Variance Analysis, 47, 583–621, https://doi.org/10.1080/01621459.1952.10483441, 1952.

Lennon, J. T. and Jones, S. E.: Microbial seed banks: the ecological and evolutionary implications of dormancy, 9, 119–130, 2011.

León-Sobrino, C., Ramond, J. B., Maggs-Kölling, G., and Cowan, D. A.: Nutrient acquisition, rather than stress response over diel cycles, drives microbial transcription in a hyper-arid Namib desert soil, 10, 1–11, https://doi.org/10.3389/fmicb.2019.01054, 2019.

Leung, P. M., Bay, S. K., Meier, D. v., Chiri, E., Cowan, D. A., Gillor, O., Woebken, D., and Greening, C.: Energetic Basis of Microbial Growth and Persistence in Desert Ecosystems, 5, 1–14, https://doi.org/10.1128/msystems.00495-19, 2020.

Mager, D. M. and Thomas, A. D.: Extracellular polysaccharides from cyanobacterial soil crusts: A review of their role in dryland soil processes, 75, 91–97, https://doi.org/10.1016/j.jaridenv.2010.10.001, 2011.

Malek, E., McCurdy, G., and Giles, B.: Dew contribution to the annual water balances in semi-arid desert valleys, 42, 71–80, https://doi.org/10.1006/jare.1999.0506, 1999.

Mazor, G., Kidron, G. J., Vonshak, A., and Abeliovich, A.: The role of cyanobacterial exopolysaccharides in structuring desert microbial crusts, 21, 121–130, https://doi.org/10.1016/0168-6496(96)00050-5, 1996.

McMurdie, P. J., Holmes, S., Jordan, G., and Chamberlain, S.: Phyloseq: handling and analysis of high-throughput microbiome census data, 2017.

Meier, D. v, Imminger, S., Gillor, O., and Woebken, D.: Versatility of energy metabolism and drought survival strategies characterize microbial genomes in biological soil crust, 2020.

Meier, D. v., Imminger, S., Gillor, O., and Woebken, D.: Distribution of Mixotrophy and Desiccation Survival Mechanisms across Microbial Genomes in an Arid Biological Soil Crust Community, 6, 1–20, https://doi.org/10.1128/msystems.00786-20, 2021.

Murik, O., Oren, N., Shotland, Y., Raanan, H., Treves, H., Kedem, I., Keren, N., Hagemann, M., Pade, N., and Kaplan, A.: What distinguishes cyanobacteria able to revive after desiccation from those that cannot: the genome aspect, 19, 535–550, https://doi.org/10.1111/1462-2920.13486, 2017.

Murrell, P.: grid Graphics Creating and Controlling Graphics Regions and Co- ordinate Systems, 1–17, https://doi.org/doi:10.1201/b10966-6, 2004.

Narayan, N. R., Weinmaier, T., Laserna-Mendieta, E. J., Claesson, M. J., Shanahan, F., Dabbagh, K., Iwai, S., and Desantis, T. Z.: Piphillin predicts metagenomic composition and dynamics from DADA2- corrected 16S rDNA sequences, 21, 1–12, https://doi.org/10.1186/s12864-020-6537-9, 2020.

Oksanen, J., Blanchet, F. G., Kindt, R., Legen-, P., Minchin, P. R., Hara, R. B. O., Simpson, G. L., Solymos, P., and Stevens, M. H. H.: Package ‘ vegan ,’ https://doi.org/ISBN 0-387-95457-0, 2014.

Oren, N., Raanan, H., Murik, O., Keren, N., and Kaplan, A.: Dawn illumination prepares desert cyanobacteria for dehydration, 27, R1056–R1057, https://doi.org/10.1016/j.cub.2017.08.027, 2017.

Oren, N., Raanan, H., Kedem, I., Turjeman, A., Bronstein, M., Kaplan, A., and Murik, O.: Desert cyanobacteria prepare in advance for dehydration and rewetting: The role of light and temperature sensing, 28, 2305–2320, https://doi.org/10.1111/mec.15074, 2019.

Péli, E. R., Lei, N., Pócs, T., Laufer, Z., Porembski, S., and Tuba, Z.: Ecophysiological responses of desiccation-tolerant cryptobiotic crusts, 6, 838–849, https://doi.org/10.2478/s11535-011-0049-1, 2011.

Pointing, S. B. and Belnap, J.: Microbial colonization and controls in dryland systems, 10, 551–562, https://doi.org/10.1038/nrmicro2831, 2012.

Preiss, J.: Bacterial glycogen synthesis and its regulation, 38, 419–458, 1984.

Preiss, J. and Sivak, M.: 3.14 - Starch and Glycogen Biosynthesis, edited by: Barton, S. D., Nakanishi, K., and Meth-Cohn, O. B. T.-C. N. P. C., Pergamon, Oxford, 441–495, https://doi.org/https://doi.org/10.1016/B978-0-08-091283-7.00082-5, 1999.

Quast, C., Pruesse, E., Yilmaz, P., Gerken, J., Schweer, T., Yarza, P., Peplies, J., and Glöckner, F. O.: The SILVA ribosomal RNA gene database project: improved data processing and web-based tools, 41, D590–D596, https://doi.org/10.1093/nar/gks1219, 2013.

Rajeev, L., da Rocha, U. N., Klitgord, N., Luning, E. G., Fortney, J., Axen, S. D., Shih, P. M., Bouskill, N. J., Bowen, B. P., Kerfeld, C. A., Garcia-Pichel, F., Brodie, E. L., Northen, T. R., and Mukhopadhyay, A.: Dynamic cyanobacterial response to hydration and dehydration in a desert biological soil crust, 7, 2178–2191, https://doi.org/10.1038/ismej.2013.83, 2013.

Repar, J., Briski, N., Buljubašić, M., Zahradka, K., and Zahradka, D.: Exonuclease VII is involved in “reckless” DNA degradation in UV-irradiated Escherichia coli, 750, https://doi.org/10.1016/j.mrgentox.2012.10.005, 2012.

Ritchie, R. J.: Consistent sets of spectrophotometric chlorophyll equations for acetone, methanol and ethanol solvents, 89, 27–41, https://doi.org/10.1007/s11120-006-9065-9, 2006.

Roberson, E. B. and Firestone, M. K.: Relationship between desiccation and exopolysaccharide production in a soil Pseudomonas sp., 58, 1284–1291, https://doi.org/10.1128/aem.58.4.1284-1291.1992, 1992.

Scrimgeour, C.: Soil Sampling and Methods of Analysis (Second Edition), edited by: Carter, M. R. and Gregorich, E. G., 1224 pp., https://doi.org/10.1017/s0014479708006546, 2008.

Sklarz, M. Y., Levin, L., Gordon, M., and Chalifa-Caspi, V.: NeatSeq-Flow: A Lightweight High Throughput Sequencing Workflow Platform for Non-Programmers and Programmers alike, 173005, https://doi.org/10.1101/173005, 2018.

Slade, D. and Radman, M.: Oxidative Stress Resistance in Deinococcus radiodurans, 133–191 pp., https://doi.org/10.1128/mmbr.00015-10, 2011.

https://doi.org/10.5194/soil-2021-88
Preprint. Discussion started: 1 September 2021

Šťovíček, A., Kim, M., Or, D., and Gillor, O.: Microbial community response to hydration-desiccation cycles in desert soil, 7, 45735, https://doi.org/10.1038/srep45735, 2017.
Sukenik, A., Kaplan-Levy, R. N., Welch, J. M., and Post, A. F.: Massive multiplication of genome and ribosomes in dormant cells (akinetes) of Aphanizomenon ovalisporum (Cyanobacteria), 6, 670–679, https://doi.org/10.1038/ismej.2011.128, 2012.
Sunyer-Figueres, M., Wang, C., and Mas, A.: Analysis of ribosomal RNA stability in dead cells of wine yeast by quantitative PCR, 270, 1–4, https://doi.org/10.1016/j.ijfoodmicro.2018.01.020, 2018.
Tveit, A. T., Hestnes, A. G., Robinson, S. L., Schintlmeister, A., Dedysh, S. N., Jehmlich, N., von Bergen, M., Herbold, C., Wagner, M., Richter, A., and Svenning, M. M.: Widespread soil bacterium that oxidizes atmospheric methane, 116, 8515–8524, https://doi.org/10.1073/pnas.1817812116, 2019.
Wickham, H.: Ggplot2: Elegant graphics for data analysis, 2016.
Wickham, H.: R: Package ‘scales,’ https://cran.r-project.org/web/packages/scales/scales.pdf, 2017.
Wickham, H. and Bache, S. M.: Magrittr: A forward-pipe operator for R, 2014.
Wickham, H., Francois, R., Henry, L., and Müller, K.: Package “dplyr,” 2018.
Wu, Y., Rao, B., Wu, P., Liu, Y., Li, G., and Li, D.: Development of artificially induced biological soil crusts in fields and their effects on topsoil, 370, 115–124, https://doi.org/10.1007/s11104-013-1611-6, 2013.
Zvyagintsev, D. G., Zenova, G. M., Doroshenko, E. A., Gryadunova, A. A., Gracheva, T. A., and Sudnitsyn, I. I.: Actinomycete growth in conditions of low moisture, 34, 242–247, https://doi.org/10.1134/S1062359007030053, 2007.

https://doi.org/10.5194/soil-2021-88
Preprint. Discussion started: 1 September 2021

APPPENDICES

APPPENDIX A

Tables

Table A1. Primers used in this study

	Primer name	Primers (5' – 3')	Reference
16S rRNA	V3F(341)	CCTACGGGAGGCAGCAG	(Klindworth et al., 2013)
	V4R(515)	TTACCGCGGCKGCTGGCAC	
	V4R(806)	GGACTACHVGGGTWTCTAAT	
Universal tags	CS1	ACACTGACGACATGGTTCTACA	
	CS2	TACGGTAGCAGAGACTTGGTCT	

https://doi.org/10.5194/soil-2021-88
Preprint. Discussion started: 1 September 2021

Table A2. Statistics from Dada2

Sample	Input	Filtered	Percentage of input passed filter	Denoised	Non-chimeric	Percentage of input non-chimeric
T[R]	99090	87403	88.21	76272	68762	69
T[R]	102014	87207	85.49	75796	64954	64
T[R]	107763	94407	87.61	80242	72676	67
T[R]	94175	81352	86.38	69460	61519	65
T[R]	97752	85658	87.63	76694	65590	67
T[1]	102147	89670	87.79	79436	68611	67
T[1]	110406	96638	87.53	86745	76384	69
T[1]	94247	81576	86.56	72289	65755	70
T[1]	107731	94180	87.42	83504	72831	68
T[1]	96982	84993	87.64	77197	67547	70
T[2]	95525	82453	86.32	73811	63892	67
T[2]	90500	79303	87.63	75977	74636	82
T[2]	84648	74376	87.87	71060	69017	82
T[2]	96778	85143	87.98	75971	66483	69
T[2]	83749	72395	86.44	65649	60857	73
T[3]	85527	74977	87.66	66324	56872	67
T[3]	92648	81056	87.49	74512	67015	72
T[3]	98388	86526	87.94	78048	69910	71
T[3]	92219	79938	86.68	69799	62666	68
T[3]	88140	77515	87.95	73273	72113	82
T[0]	22095	21646	97.97	19900	12628	57
T[0]	23457	22888	97.57	18342	11627	50
T[0]	26072	25368	97.30	20726	12867	49

https://doi.org/10.5194/soil-2021-88
Preprint. Discussion started: 1 September 2021

Table A3. List of the genes used for function prediction ordered by groups and subgroups.

Group	Metabolic traits	KEGG ID	Function
DNA conservation	Putative DNA-binding protein	K02524	K10; DNA binding protein (fs(1)K10, female sterile(1)K10)
	Putative DNA-binding protein	K03111	ssb; single-strand DNA-binding protein
	Putative DNA-binding protein	K03530	hupB; DNA-binding protein HU-beta
	Putative DNA-binding protein	K03622	ssh10b; archaea-specific DNA-binding protein
	Putative DNA-binding protein	K03746	hns; DNA-binding protein H-NS
	Putative DNA-binding protein	K04047	dps; starvation-inducible DNA-binding protein
	Putative DNA-binding protein	K04494	CHD8, HELSNF1; chromodomain helicase DNA binding protein 8 [EC:3.6.4.12]
	Putative DNA-binding protein	K04680	ID1; DNA-binding protein inhibitor ID1
	Putative DNA-binding protein	K05516	cbpA; curved DNA-binding protein
	Putative DNA-binding protein	K05732	ARHGAP35, GRLF1; glucocorticoid receptor DNA-binding factor 1
	Putative DNA-binding protein	K05787	hupA; DNA-binding protein HU-alpha
	Putative DNA-binding protein	K09061	GCF, C2orf3; GC-rich sequence DNA-binding factor
	Putative DNA-binding protein	K09423	BAS1; Myb-like DNA-binding protein BAS1
	Putative DNA-binding protein	K09424	REB1; Myb-like DNA-binding protein REB1
	Putative DNA-binding protein	K09425	K09425; Myb-like DNA-binding protein FlbD
	Putative DNA-binding protein	K09426	RAP1; Myb-like DNA-binding protein RAP1
	Putative DNA-binding protein	K10140	DDB2; DNA damage-binding protein 2
	Putative DNA-binding protein	K10610	DDB1; DNA damage-binding protein 1
	Putative DNA-binding protein	K10728	TOPBP1; topoisomerase (DNA) II binding protein 1
	Putative DNA-binding protein	K10748	tus, tau; DNA replication terminus site-binding protein
	Histone-like protein	K10752	RBBP4, HAT2, CAF1, MIS16; histone-binding protein RBBP4
	Putative DNA-binding protein	K10979	ku; DNA end-binding protein Ku
	Putative DNA-binding protein	K11367	CHD1; chromodomain-helicase-DNA-binding protein 1 [EC:3.6.4.12]
	Histone-like protein	K11495	CENPA; histone H3-like centromeric protein A

https://doi.org/10.5194/soil-2021-88
Preprint. Discussion started: 1 September 2021

	Putative DNA-binding protein	K11574	CBF2, CBF3A, CTF14; centromere DNA-binding protein complex CBF3 subunit A
	Putative DNA-binding protein	K11575	CEP3, CBF3B; centromere DNA-binding protein complex CBF3 subunit B
	Putative DNA-binding protein	K11576	CTF13, CBF3C; centromere DNA-binding protein complex CBF3 subunit C
	Putative DNA-binding protein	K11642	CHD3, MI2A; chromodomain-helicase-DNA-binding protein 3 [EC:3.6.4.12]
	Putative DNA-binding protein	K11643	CHD4, MI2B; chromodomain-helicase-DNA-binding protein 4 [EC:3.6.4.12]
	Histone-like protein	K11659	RBBP7; histone-binding protein RBBP7
	Putative DNA-binding protein	K11685	stpA; DNA-binding protein StpA
	Putative DNA-binding protein	K12965	ZBP1, DAI; Z-DNA binding protein 1
	Putative DNA-binding protein	K13102	KIN; DNA/RNA-binding protein KIN17
	Putative DNA-binding protein	K13211	GCFC; GC-rich sequence DNA-binding factor
	Putative DNA-binding protein	K14435	CHD5; chromodomain-helicase-DNA-binding protein 5 [EC:3.6.4.12]
	Putative DNA-binding protein	K14436	CHD6; chromodomain-helicase-DNA-binding protein 6 [EC:3.6.4.12]
	Putative DNA-binding protein	K14437	CHD7; chromodomain-helicase-DNA-binding protein 7 [EC:3.6.4.12]
	Putative DNA-binding protein	K14438	CHD9; chromodomain-helicase-DNA-binding protein 9 [EC:3.6.4.12]
	Putative DNA-binding protein	K14507	ORCA2_3; AP2-domain DNA-binding protein ORCA2/3
	Histone-like protein	K15719	NCOAT, MGEA5; protein O-GlcNAcase / histone acetyltransferase [EC:3.2.1.169 2.3.1.48]
	Putative DNA-binding protein	K16640	ssh7; DNA-binding protein 7 [EC:3.1.27.-]
	Putative DNA-binding protein	K17693	ID2; DNA-binding protein inhibitor ID2
	Putative DNA-binding protein	K17694	ID3; DNA-binding protein inhibitor ID3
	Putative DNA-binding protein	K17695	ID4; DNA-binding protein inhibitor ID4
	Putative DNA-binding protein	K17696	EMC; DNA-binding protein inhibitor ID, other
	Histone-like protein	K18710	SLBP; histone RNA hairpin-binding protein
	Putative DNA-binding protein	K18946	gp32, ssb; single-stranded DNA-binding protein
	Putative DNA-binding protein	K19442	ICP8, DBP, UL29; Simplexvirus major DNA-binding protein
	Histone-like protein	K19799	RPH1; DNA damage-responsive transcriptional repressor / [histone H3]-trimethyl-L-lysine36 demethylase [EC:1.14.11.69]
	Putative DNA-binding protein	K20091	CHD2; chromodomain-helicase-DNA-binding protein 2 [EC:3.6.4.12]

https://doi.org/10.5194/soil-2021-88
Preprint. Discussion started: 1 September 2021

	Putative DNA-binding protein	K20092	CHD1L; chromodomain-helicase-DNA-binding protein 1-like [EC:3.6.4.12]
	Putative DNA-binding protein	K22592	AHDC1; AT-hook DNA-binding motif-containing protein 1
	Putative DNA-binding protein	K23225	SATB1; DNA-binding protein SATB1
	Putative DNA-binding protein	K23226	SATB2; DNA-binding protein SATB2
	Putative DNA-binding protein	K23600	TARDBP, TDP43; TAR DNA-binding protein 43
DNA repair	DNA polymerase PolA (COG0258)	K02320	POLA1; DNA polymerase alpha subunit A [EC:2.7.7.7]
	DNA polymerase PolA (COG0258)	K02321	POLA2; DNA polymerase alpha subunit B
	DNA polymerase PolA (COG0258)	K02335	polA; DNA polymerase I [EC:2.7.7.7]
	DNA polymerase IV	K02346	dinB; DNA polymerase IV [EC:2.7.7.7]
	Exodeoxyribonuclease VII	K03601	xseA; exodeoxyribonuclease VII large subunit [EC:3.1.11.6]
	Exodeoxyribonuclease VII	K03602	xseB; exodeoxyribonuclease VII small subunit [EC:3.1.11.6]
	DNA polymerase IV	K04479	dbh; DNA polymerase IV (archaeal DinB-like DNA polymerase) [EC:2.7.7.7]
	Exodeoxyribonuclease VII	K10906	recE; exodeoxyribonuclease VIII [EC:3.1.11.-]
	DNA polymerase IV	K10981	POL4; DNA polymerase IV [EC:2.7.7.7]
	DNA polymerase IV	K16250	NRPD1; DNA-directed RNA polymerase IV subunit 1 [EC:2.7.7.6]
	DNA polymerase IV	K16252	NRPD2, NRPE2; DNA-directed RNA polymerase IV and V subunit 2 [EC:2.7.7.6]
	DNA polymerase IV	K16253	NRPD7, NRPE7; DNA-directed RNA polymerase IV and V subunit 7
Lithotrophy	NiFe hydrogenase	K00437	hydB ; [NiFe] hydrogenase large subunit [EC:1.12.2.1]
	NiFe hydrogenase	K02587	nifE; nitrogenase molybdenum-cofactor synthesis protein NifE
	CO-dehydrogenase CoxM & CoxS	K03518	coxS; aerobic carbon-monoxide dehydrogenase small subunit [EC:1.2.5.3]
	CO-dehydrogenase CoxM & CoxS	K03519	coxM, cutM; aerobic carbon-monoxide dehydrogenase medium subunit [EC:1.2.5.3]
	CO-dehydrogenase large subunit (coxL) Form I	K03520	CoxL, cutL; aerobic carbon-monoxide dehydrogenase large subunit [EC:1.2.5.3]
	NiFe hydrogenase	K05586	hoxE ; bidirectional [NiFe] hydrogenase diaphorase subunit [EC:7.1.1.2]
	NiFe hydrogenase	K05587	hoxF; bidirectional [NiFe] hydrogenase diaphorase subunit [EC:7.1.1.2]
	NiFe hydrogenase	K05588	hoxU ; bidirectional [NiFe] hydrogenase diaphorase subunit [EC:7.1.1.2]
	SOX sulfur-oxidation system	K17218	sqr; sulfide:quinone oxidoreductase [EC:1.8.5.4]

https://doi.org/10.5194/soil-2021-88
Preprint. Discussion started: 1 September 2021

	SOX sulfur-oxidation system	K17222	soxA; L-cysteine S-thiosulfotransferase [EC:2.8.5.2]
	SOX sulfur-oxidation system	K17223	soxX; L-cysteine S-thiosulfotransferase [EC:2.8.5.2]
	SOX sulfur-oxidation system	K17224	soxB; S-sulfosulfanyl-L-cysteine sulfohydrolase [EC:3.1.6.20]
	SOX sulfur-oxidation system	K17225	soxC ; sulfane dehydrogenase subunit SoxC
	SOX sulfur-oxidation system	K17226	soxY; sulfur-oxidizing protein SoxY
	SOX sulfur-oxidation system	K17227	soxZ; sulfur-oxidizing protein SoxZ
	NiFe hydrogenase	K18005	hoxF; [NiFe] hydrogenase diaphorase moiety large subunit [EC:1.12.1.2]
	NiFe hydrogenase	K18006	hoxU; [NiFe] hydrogenase diaphorase moiety small subunit [EC:1.12.1.2]
	NiFe hydrogenase	K18008	hydA; [NiFe] hydrogenase small subunit [EC:1.12.2.1]
	Propane monooxygenase (soluble)	K18223	prmA ; propane 2-monooxygenase large subunit [EC:1.14.13.227]
	Propane monooxygenase (soluble)	K18224	prmC; propane 2-monooxygenase small subunit [EC:1.14.13.227]
	Propane monooxygenase (soluble)	K18225	prmB; propane monooxygenase reductase component [EC:1.18.1.-]
	Propane monooxygenase (soluble)	K18226	prmD; propane monooxygenase coupling protein
	SOX sulfur-oxidation system	K22622	soxD; S-disulfanyl-L-cysteine oxidoreductase SoxD [EC:1.8.2.6]
	SOX sulfur-oxidation system	K24007	soxD; cytochrome aa3-type oxidase subunit SoxD
	SOX sulfur-oxidation system	K24008	soxC; cytochrome aa3-type oxidase subunit III
	SOX sulfur-oxidation system	K24009	soxB; cytochrome aa3-type oxidase subunit I [EC:7.1.1.4]
	SOX sulfur-oxidation system	K24010	soxA; cytochrome aa3-type oxidase subunit II [EC:7.1.1.4]
	SOX sulfur-oxidation system	K24011	soxM; cytochrome aa3-type oxidase subunit I/III [EC:7.1.1.4]
Organotrophy	ABC sugar transporters	K02025	ABC.MS.P; multiple sugar transport system permease protein
	ABC sugar transporters	K02026	ABC.MS.P1; multiple sugar transport system permease protein
	ABC sugar transporters	K02027	ABC.MS.S; multiple sugar transport system substrate-binding protein
	ABC sugar transporters	K02056	ABC.SS.A; simple sugar transport system ATP-binding protein [EC:7.5.2.-]
	ABC sugar transporters	K02057	ABC.SS.P; simple sugar transport system permease protein
	ABC sugar transporters	K02058	ABC.SS.S; simple sugar transport system substrate-binding protein

https://doi.org/10.5194/soil-2021-88
Preprint. Discussion started: 1 September 2021

	PTS sugar importers	K02777	crr; sugar PTS system EIIA component [EC:2.7.1.-]
	Amino acid transporter	K03293	TC.AAT; amino acid transporter, AAT family
	Peptide transporter	K03305	TC.POT; proton-dependent oligopeptide transporter, POT family
	Amino acid transporter	K03311	TC.LIVCS; branched-chain amino acid:cation transporter, LIVCS family
	Carboxylate transporters	K03326	TC.DCUC, dcuC, dcuD; C4-dicarboxylate transporter, DcuC family
	Amino acid transporter	K03450	SLC7A; solute carrier family 7 (L-type amino acid transporter), other
	Glycosyl hydrolases	K04844	ycjT; hypothetical glycosyl hydrolase [EC:3.2.1.-]
	Amino acid transporter	K05048	SLC6A15S; solute carrier family 6 (neurotransmitter transporter, amino acid/orphan) member 15/16/17/18/20
	Amino acid transporter	K05615	SLC1A4, SATT; solute carrier family 1 (neutral amino acid transporter), member 4
	Amino acid transporter	K05616	SLC1A5; solute carrier family 1 (neutral amino acid transporter), member 5
	Amino acid transporter	K07084	yuiF; putative amino acid transporter
	Carboxylate transporters	K07791	dcuA ; anaerobic C4-dicarboxylate transporter DcuA
	Carboxylate transporters	K07792	dcuB; anaerobic C4-dicarboxylate transporter DcuB
	ABC sugar transporters	K10546	ABC.GGU.S, chvE; putative multiple sugar transport system substrate-binding protein
	ABC sugar transporters	K10547	ABC.GGU.P, gguB; putative multiple sugar transport system permease protein
	ABC sugar transporters	K10548	ABC.GGU.A, gguA; putative multiple sugar transport system ATP-binding protein [EC:7.5.2.-]
	Carboxylate transporters	K11689	dctQ ; C4-dicarboxylate transporter, DctQ subunit
	Carboxylate transporters	K11690	dctM; C4-dicarboxylate transporter, DctM subunit
	Amino acid transporter	K13576	SLC38A3, SNAT3; solute carrier family 38 (sodium-coupled neutral amino acid transporter), member 3
	Carboxylate transporters	K13577	SLC25A10, DIC; solute carrier family 25 (mitochondrial dicarboxylate transporter), member 10
	Amino acid transporter	K13780	SLC7A5, LAT1; solute carrier family 7 (L-type amino acid transporter), member 5
	Amino acid transporter	K13781	SLC7A8, LAT2; solute carrier family 7 (L-type amino acid transporter), member 8
	Amino acid transporter	K13782	SLC7A10, ASC1; solute carrier family 7 (L-type amino acid transporter), member 10
	Amino acid transporter	K13863	SLC7A1, ATRC1; solute carrier family 7 (cationic amino acid transporter), member 1
	Amino acid transporter	K13864	SLC7A2, ATRC2; solute carrier family 7 (cationic amino acid transporter), member 2

https://doi.org/10.5194/soil-2021-88
Preprint. Discussion started: 1 September 2021

	Amino acid transporter	K13865	SLC7A3, ATRC3; solute carrier family 7 (cationic amino acid transporter), member 3
	Amino acid transporter	K13866	SLC7A4; solute carrier family 7 (cationic amino acid transporter), member 4
	Amino acid transporter	K13867	SLC7A7; solute carrier family 7 (L-type amino acid transporter), member 7
	Amino acid transporter	K13868	SLC7A9, BAT1; solute carrier family 7 (L-type amino acid transporter), member 9
	Amino acid transporter	K13869	SLC7A11; solute carrier family 7 (L-type amino acid transporter), member 11
	Amino acid transporter	K13870	SLC7A13, AGT1; solute carrier family 7 (L-type amino acid transporter), member 13
	Amino acid transporter	K13871	SLC7A14; solute carrier family 7 (cationic amino acid transporter), member 14
	Amino acid transporter	K13872	SLC7A6; solute carrier family 7 (L-type amino acid transporter), member 6
	Peptide transporter	K14206	SLC15A1, PEPT1; solute carrier family 15 (oligopeptide transporter), member 1
	Amino acid transporter	K14207	SLC38A2, SNAT2; solute carrier family 38 (sodium-coupled neutral amino acid transporter), member 2
	Amino acid transporter	K14209	SLC36A, PAT; solute carrier family 36 (proton-coupled amino acid transporter)
	Amino acid transporter	K14210	SLC3A1, RBAT; solute carrier family 3 (neutral and basic amino acid transporter), member 1
	Carboxylate transporters	K14388	SLC5A8_12, SMCT; solute carrier family 5 (sodium-coupled monocarboxylate transporter), member 8/12
	Carboxylate transporters	K14445	SLC13A2_3_5; solute carrier family 13 (sodium-dependent dicarboxylate transporter), member 2/3/5
	Peptide transporter	K14637	SLC15A2, PEPT2; solute carrier family 15 (oligopeptide transporter), member 2
	Peptide transporter	K14638	SLC15A3_4, PHT; solute carrier family 15 (peptide/histidine transporter), member 3/4
	Amino acid transporter	K14990	SLC38A1, SNAT1, GLNT; solute carrier family 38 (sodium-coupled neutral amino acid transporter), member 1
	Amino acid transporter	K14991	SLC38A4, SNAT4; solute carrier family 38 (sodium-coupled neutral amino acid transporter), member 4
	Amino acid transporter	K14992	SLC38A5, SNAT5; solute carrier family 38 (sodium-coupled neutral amino acid transporter), member 5
	Amino acid transporter	K14993	SLC38A6, SNAT6; solute carrier family 38 (sodium-coupled neutral amino acid transporter), member 6
	Amino acid transporter	K14994	SLC38A7_8; solute carrier family 38 (sodium-coupled neutral amino acid transporter), member 7/8
	Amino acid transporter	K14995	SLC38A9; solute carrier family 38 (sodium-coupled neutral amino acid transporter), member 9

https://doi.org/10.5194/soil-2021-88
Preprint. Discussion started: 1 September 2021

	Amino acid transporter	K14996	SLC38A10; solute carrier family 38 (sodium-coupled neutral amino acid transporter), member 10
	Amino acid transporter	K14997	SLC38A11; solute carrier family 38 (sodium-coupled neutral amino acid transporter), member 11
	Amino acid transporter	K15015	SLC32A, VGAT; solute carrier family 32 (vesicular inhibitory amino acid transporter)
	Carboxylate transporters	K15110	SLC25A21, ODC; solute carrier family 25 (mitochondrial 2-oxodicarboxylate transporter), member 21
	Amino acid transporter	K16261	YAT; yeast amino acid transporter
	Amino acid transporter	K16263	yjeH; amino acid efflux transporter
	Peptide transporter	K17938	sbmA, bacA; peptide/bleomycin uptake transporter
Phototrophy	RuBisCO	K01601	rbcL; ribulose-bisphosphate carboxylase large chain [EC:4.1.1.39]
	Chlorophyll synthesis	K01669	phrB; deoxyribodipyrimidine photo-lyase [EC:4.1.99.3]
	Chlorophyll synthesis	K02689	psaA; photosystem I P700 chlorophyll a apoprotein A1
	Chlorophyll synthesis	K02690	psaB; photosystem I P700 chlorophyll a apoprotein A2
	Chlorophyll synthesis	K02691	psaC; photosystem I subunit VII
	Chlorophyll synthesis	K02692	psaD; photosystem I subunit II
	Chlorophyll synthesis	K02693	psaE; photosystem I subunit IV
	Chlorophyll synthesis	K02694	psaF; photosystem I subunit III
	Chlorophyll synthesis	K02695	psaH; photosystem I subunit VI
	Chlorophyll synthesis	K02696	psaI; photosystem I subunit VIII
	Chlorophyll synthesis	K02697	psaJ; photosystem I subunit IX
	Chlorophyll synthesis	K02698	psaK; photosystem I subunit X
	Chlorophyll synthesis	K02699	psaL; photosystem I subunit XI
	Chlorophyll synthesis	K02700	psaM; photosystem I subunit XII
	Chlorophyll synthesis	K02701	psaN; photosystem I subunit PsaN
	Chlorophyll synthesis	K02702	psaX; photosystem I 4.8kDa protein
	Chlorophyll synthesis	K02703	psbA; photosystem II P680 reaction center D1 protein [EC:1.10.3.9]
	Chlorophyll synthesis	K02704	psbB; photosystem II CP47 chlorophyll apoprotein

https://doi.org/10.5194/soil-2021-88
Preprint. Discussion started: 1 September 2021

	Chlorophyll synthesis	K02705	psbC; photosystem II CP43 chlorophyll apoprotein
	Chlorophyll synthesis	K02706	psbD; photosystem II P680 reaction center D2 protein [EC:1.10.3.9]
	Chlorophyll synthesis	K02707	psbE; photosystem II cytochrome b559 subunit alpha
	Chlorophyll synthesis	K02708	psbF; photosystem II cytochrome b559 subunit beta
	Chlorophyll synthesis	K02709	psbH; photosystem II PsbH protein
	Chlorophyll synthesis	K02710	psbI; photosystem II PsbI protein
	Chlorophyll synthesis	K02711	psbJ; photosystem II PsbJ protein
	Chlorophyll synthesis	K02712	psbK; photosystem II PsbK protein
	Chlorophyll synthesis	K02713	psbL; photosystem II PsbL protein
	Chlorophyll synthesis	K02714	psbM; photosystem II PsbM protein
	Chlorophyll synthesis	K02716	psbO; photosystem II oxygen-evolving enhancer protein 1
	Chlorophyll synthesis	K02717	psbP; photosystem II oxygen-evolving enhancer protein 2
	Chlorophyll synthesis	K02718	psbT; photosystem II PsbT protein
	Chlorophyll synthesis	K02719	psbU; photosystem II PsbU protein
	Chlorophyll synthesis	K02720	psbV; photosystem II cytochrome c550
	Chlorophyll synthesis	K02721	psbW; photosystem II PsbW protein
	Chlorophyll synthesis	K02722	psbX; photosystem II PsbX protein
	Chlorophyll synthesis	K02723	psbY; photosystem II PsbY protein
	Chlorophyll synthesis	K02724	psbZ; photosystem II PsbZ protein
	Chlorophyll synthesis	K03157	LTB, TNFC; lymphotoxin beta (TNF superfamily, member 3)
	Chlorophyll synthesis	K03159	TNFRSF3, LTBR; lymphotoxin beta receptor TNFR superfamily member 3
	Chlorophyll synthesis	K03541	psbR; photosystem II 10kDa protein
	Chlorophyll synthesis	K03542	psbS; photosystem II 22kDa protein
	Chlorophyll synthesis	K03716	splB; spore photoproduct lyase [EC:4.1.99.14]
	Chlorophyll synthesis	K05468	LTA, TNFB; lymphotoxin alpha (TNF superfamily, member 1)
	Chlorophyll synthesis	K06315	splA; transcriptional regulator of the spore photoproduct lyase operon
	Chlorophyll synthesis	K06876	K06876; deoxyribodipyrimidine photolyase-related protein

https://doi.org/10.5194/soil-2021-88
Preprint. Discussion started: 1 September 2021

	Chlorophyll synthesis	K08901	psbQ; photosystem II oxygen-evolving enhancer protein 3
	Chlorophyll synthesis	K08902	psb27; photosystem II Psb27 protein
	Chlorophyll synthesis	K08903	psb28; photosystem II 13kDa protein
	Chlorophyll synthesis	K08904	psb28-2; photosystem II Psb28-2 protein
	Chlorophyll synthesis	K08905	psaG; photosystem I subunit V
	Chlorophyll synthesis	K08928	pufL; photosynthetic reaction center L subunit
	Chlorophyll synthesis	K08929	pufM; photosynthetic reaction center M subunit
	Chlorophyll synthesis	K08940	pscA; photosystem P840 reaction center large subunit
	Chlorophyll synthesis	K08941	pscB; photosystem P840 reaction center iron-sulfur protein
	Chlorophyll synthesis	K08942	pscC; photosystem P840 reaction center cytochrome c551
	Chlorophyll synthesis	K08943	pscD; photosystem P840 reaction center protein PscD
	Chlorophyll synthesis	K11524	pixI ; positive phototaxis protein PixI
	Chlorophyll synthesis	K13991	puhA; photosynthetic reaction center H subunit
	Chlorophyll synthesis	K13992	pufC; photosynthetic reaction center cytochrome c subunit
	Chlorophyll synthesis	K13994	pufX; photosynthetic reaction center PufX protein
	Chlorophyll synthesis	K14332	psaO; photosystem I subunit PsaO
	Chlorophyll synthesis	K19016	IMPG1, SPACR; interphotoreceptor matrix proteoglycan 1
	Chlorophyll synthesis	K19017	IMPG2, SPACRCAN; interphotoreceptor matrix proteoglycan 2
	Chlorophyll synthesis	K20715	PHOT; phototropin [EC:2.7.11.1]
	Chlorophyll synthesis	K22464	FAP; fatty acid photodecarboxylase [EC:4.1.1.106]
	Chlorophyll synthesis	K22619	Aequorin; calcium-regulated photoprotein [EC:1.13.12.24]
	Chlorophyll synthesis	K24165	PCARE; photoreceptor cilium actin regulator
ROS-damage prevention	Cytochrome C oxidase	K00404	ccoN; cytochrome c oxidase cbb3-type subunit I [EC:7.1.1.9]
	Cytochrome C oxidase	K00405	ccoO; cytochrome c oxidase cbb3-type subunit II
	Cytochrome C oxidase	K00406	ccoP; cytochrome c oxidase cbb3-type subunit III
	Cytochrome C oxidase	K00407	ccoQ; cytochrome c oxidase cbb3-type subunit IV
	Cytochrome bd ubiquinol oxidase	K00424	cydX; cytochrome bd-I ubiquinol oxidase subunit X [EC:7.1.1.7]

https://doi.org/10.5194/soil-2021-88
Preprint. Discussion started: 1 September 2021

	Cytochrome C oxidase	K00424	cydX; cytochrome bd-I ubiquinol oxidase subunit X [EC:7.1.1.7]
	Cytochrome bd ubiquinol oxidase	K00425	cydA; cytochrome bd ubiquinol oxidase subunit I [EC:7.1.1.7]
	Cytochrome C oxidase	K00425	cydA; cytochrome bd ubiquinol oxidase subunit I [EC:7.1.1.7]
	Cytochrome bd ubiquinol oxidase	K00426	cydB; cytochrome bd ubiquinol oxidase subunit II [EC:7.1.1.7]
	Cytochrome C oxidase	K00426	cydB; cytochrome bd ubiquinol oxidase subunit II [EC:7.1.1.7]
	Cytochrome C oxidase	K00428	E1.11.1.5; cytochrome c peroxidase [EC:1.11.1.5]
	Cytochrome C oxidase	K02256	COX1; cytochrome c oxidase subunit 1 [EC:7.1.1.9]
	Cytochrome C oxidase	K02258	COX11, ctaG; cytochrome c oxidase assembly protein subunit 11
	Cytochrome C oxidase	K02259	COX15, ctaA; cytochrome c oxidase assembly protein subunit 15
	Cytochrome C oxidase	K02260	COX17; cytochrome c oxidase assembly protein subunit 17
	Cytochrome C oxidase	K02261	COX2; cytochrome c oxidase subunit 2
	Cytochrome C oxidase	K02262	COX3; cytochrome c oxidase subunit 3
	Cytochrome C oxidase	K02263	COX4; cytochrome c oxidase subunit 4
	Cytochrome C oxidase	K02264	COX5A; cytochrome c oxidase subunit 5a
	Cytochrome C oxidase	K02265	COX5B; cytochrome c oxidase subunit 5b
	Cytochrome C oxidase	K02266	COX6A; cytochrome c oxidase subunit 6a
	Cytochrome C oxidase	K02267	COX6B; cytochrome c oxidase subunit 6b
	Cytochrome C oxidase	K02268	COX6C; cytochrome c oxidase subunit 6c
	Cytochrome C oxidase	K02269	COX7; cytochrome c oxidase subunit 7
	Cytochrome C oxidase	K02270	COX7A; cytochrome c oxidase subunit 7a
	Cytochrome C oxidase	K02271	COX7B; cytochrome c oxidase subunit 7b
	Cytochrome C oxidase	K02272	COX7C; cytochrome c oxidase subunit 7c
	Cytochrome C oxidase	K02273	COX8; cytochrome c oxidase subunit 8
	Cytochrome C oxidase	K02274	coxA, ctaD; cytochrome c oxidase subunit I [EC:7.1.1.9]
	Cytochrome C oxidase	K02275	coxB, ctaC; cytochrome c oxidase subunit II [EC:7.1.1.9]
	Cytochrome C oxidase	K02276	coxC, ctaE; cytochrome c oxidase subunit III [EC:7.1.1.9]
	Cytochrome C oxidase	K02277	coxD, ctaF; cytochrome c oxidase subunit IV [EC:7.1.1.9]

https://doi.org/10.5194/soil-2021-88
Preprint. Discussion started: 1 September 2021

	Cytochrome C oxidase	K02297	cyoA; cytochrome o ubiquinol oxidase subunit II [EC:7.1.1.3]
	Cytochrome C oxidase	K02298	cyoB; cytochrome o ubiquinol oxidase subunit I [EC:7.1.1.3]
	Cytochrome C oxidase	K02299	cyoC; cytochrome o ubiquinol oxidase subunit III
	Cytochrome C oxidase	K02300	cyoD; cytochrome o ubiquinol oxidase subunit IV
	Cytochrome C oxidase	K02826	qoxA ; cytochrome aa3-600 menaquinol oxidase subunit II [EC:7.1.1.5]
	Cytochrome C oxidase	K02827	qoxB; cytochrome aa3-600 menaquinol oxidase subunit I [EC:7.1.1.5]
	Cytochrome C oxidase	K02828	qoxC; cytochrome aa3-600 menaquinol oxidase subunit III [EC:7.1.1.5]
	Cytochrome C oxidase	K02829	qoxD; cytochrome aa3-600 menaquinol oxidase subunit IV [EC:7.1.1.5]
	Mn2+ catalase	K07217	K07217; Mn-containing catalase
	Cytochrome C oxidase	K15408	coxAC; cytochrome c oxidase subunit I+III [EC:7.1.1.9]
	Cytochrome C oxidase	K15862	ccoNO; cytochrome c oxidase cbb3-type subunit I/II [EC:7.1.1.9]
	Cytochrome C oxidase	K18173	COA1; cytochrome c oxidase assembly factor 1
	Cytochrome C oxidase	K18174	COA2; cytochrome c oxidase assembly factor 2
	Cytochrome C oxidase	K18175	CCDC56, COA3; cytochrome c oxidase assembly factor 3, animal type
	Cytochrome C oxidase	K18176	COA3; cytochrome c oxidase assembly factor 3, fungi type
	Cytochrome C oxidase	K18177	COA4; cytochrome c oxidase assembly factor 4
	Cytochrome C oxidase	K18178	COA5, PET191; cytochrome c oxidase assembly factor 5
	Cytochrome C oxidase	K18179	COA6; cytochrome c oxidase assembly factor 6
	Cytochrome C oxidase	K18180	COA7, SELRC1, RESA1; cytochrome c oxidase assembly factor 7
	Cytochrome C oxidase	K18181	COX14; cytochrome c oxidase assembly factor 14
	Cytochrome C oxidase	K18182	COX16; cytochrome c oxidase assembly protein subunit 16
	Cytochrome C oxidase	K18183	COX19; cytochrome c oxidase assembly protein subunit 19
	Cytochrome C oxidase	K18184	COX20; cytochrome c oxidase assembly protein subunit 20
	Cytochrome C oxidase	K18185	COX23; cytochrome c oxidase assembly protein subunit 23
	Cytochrome C oxidase	K18189	TACO1; translational activator of cytochrome c oxidase 1
	Cytochrome bd ubiquinol oxidase	K22501	appX; cytochrome bd-II ubiquinol oxidase subunit AppX [EC:7.1.1.7]
	Cytochrome C oxidase	K22501	appX; cytochrome bd-II ubiquinol oxidase subunit AppX [EC:7.1.1.7]

https://doi.org/10.5194/soil-2021-88
Preprint. Discussion started: 1 September 2021

	Cytochrome C oxidase	K24007	soxD; cytochrome aa3-type oxidase subunit SoxD
	Cytochrome C oxidase	K24008	soxC; cytochrome aa3-type oxidase subunit III
	Cytochrome C oxidase	K24009	soxB; cytochrome aa3-type oxidase subunit I [EC:7.1.1.4]
	Cytochrome C oxidase	K24010	soxA; cytochrome aa3-type oxidase subunit II [EC:7.1.1.4]
	Cytochrome C oxidase	K24011	soxM; cytochrome aa3-type oxidase subunit I/III [EC:7.1.1.4]
Sporulation	Glycogen synthesis	K00693	GYS; glycogen synthase [EC:2.4.1.11]
	Sporulation (Actinobacteria)	K02490	spo0F; two-component system, response regulator, stage 0 sporulation protein F
	Sporulation (Actinobacteria)	K02491	kinA; two-component system, sporulation sensor kinase A [EC:2.7.13.3]
	Glycogen synthesis	K03083	GSK3B; glycogen synthase kinase 3 beta [EC:2.7.11.26]
	Sporulation (Actinobacteria)	K03091	sigH; RNA polymerase sporulation-specific sigma factor
	Sporulation (Actinobacteria)	K04769	spoVT; AbrB family transcriptional regulator, stage V sporulation protein T
	Sporulation (Actinobacteria)	K06283	spoIIID; putative DeoR family transcriptional regulator, stage III sporulation protein D
	Sporulation (Actinobacteria)	K06348	kapD; sporulation inhibitor KapD
	Sporulation (Actinobacteria)	K06359	rapA, spo0L; response regulator aspartate phosphatase A (stage 0 sporulation protein L) [EC:3.1.-.-]
	Sporulation (Actinobacteria)	K06371	sda; developmental checkpoint coupling sporulation initiation to replication initiation
	Sporulation (Actinobacteria)	K06375	spo0B; stage 0 sporulation protein B (sporulation initiation phosphotransferase) [EC:2.7.-.-]
	Sporulation (Actinobacteria)	K06376	spo0E; stage 0 sporulation regulatory protein
	Sporulation (Actinobacteria)	K06377	spo0M; sporulation-barren protein
	Sporulation (Actinobacteria)	K06378	spoIIAA; stage II sporulation protein AA (anti-sigma F factor antagonist)
	Sporulation (Actinobacteria)	K06379	spoIIAB; stage II sporulation protein AB (anti-sigma F factor) [EC:2.7.11.1]
	Sporulation (Actinobacteria)	K06380	spoIIB; stage II sporulation protein B
	Sporulation (Actinobacteria)	K06381	spoIID; stage II sporulation protein D
	Sporulation (Actinobacteria)	K06382	spoIIE; stage II sporulation protein E [EC:3.1.3.16]
	Sporulation (Actinobacteria)	K06383	spoIIGA; stage II sporulation protein GA (sporulation sigma-E factor processing peptidase) [EC:3.4.23.-]
	Sporulation (Actinobacteria)	K06384	spoIIM; stage II sporulation protein M

https://doi.org/10.5194/soil-2021-88
Preprint. Discussion started: 1 September 2021

	Sporulation (Actinobacteria)	K06385	spoIIP; stage II sporulation protein P
	Sporulation (Actinobacteria)	K06386	spoIIQ ; stage II sporulation protein Q
	Sporulation (Actinobacteria)	K06387	spoIIR; stage II sporulation protein R
	Sporulation (Actinobacteria)	K06388	spoIISA ; stage II sporulation protein SA
	Sporulation (Actinobacteria)	K06389	spoIISB; stage II sporulation protein SB
	Sporulation (Actinobacteria)	K06390	spoIIIAA; stage III sporulation protein AA
	Sporulation (Actinobacteria)	K06391	spoIIIAB; stage III sporulation protein AB
	Sporulation (Actinobacteria)	K06392	spoIIIAC; stage III sporulation protein AC
	Sporulation (Actinobacteria)	K06393	spoIIIAD; stage III sporulation protein AD
	Sporulation (Actinobacteria)	K06394	spoIIIAE; stage III sporulation protein AE
	Sporulation (Actinobacteria)	K06395	spoIIIAF; stage III sporulation protein AF
	Sporulation (Actinobacteria)	K06396	spoIIIAG; stage III sporulation protein AG
	Sporulation (Actinobacteria)	K06397	spoIIIAH; stage III sporulation protein AH
	Sporulation (Actinobacteria)	K06398	spoIVA; stage IV sporulation protein A
	Sporulation (Actinobacteria)	K06399	spoIVB; stage IV sporulation protein B [EC:3.4.21.116]
	Sporulation (Actinobacteria)	K06401	spoIVFA; stage IV sporulation protein FA
	Sporulation (Actinobacteria)	K06402	spoIVFB; stage IV sporulation protein FB [EC:3.4.24.-]
	Sporulation (Actinobacteria)	K06403	spoVAA; stage V sporulation protein AA
	Sporulation (Actinobacteria)	K06404	spoVAB; stage V sporulation protein AB
	Sporulation (Actinobacteria)	K06405	spoVAC; stage V sporulation protein AC
	Sporulation (Actinobacteria)	K06406	spoVAD; stage V sporulation protein AD
	Sporulation (Actinobacteria)	K06407	spoVAE; stage V sporulation protein AE
	Sporulation (Actinobacteria)	K06408	spoVAF; stage V sporulation protein AF
	Sporulation (Actinobacteria)	K06409	spoVB; stage V sporulation protein B
	Sporulation (Actinobacteria)	K06412	spoVG; stage V sporulation protein G
	Sporulation (Actinobacteria)	K06413	spoVK; stage V sporulation protein K
	Sporulation (Actinobacteria)	K06414	spoVM; stage V sporulation protein M

https://doi.org/10.5194/soil-2021-88
Preprint. Discussion started: 1 September 2021

	Sporulation (Actinobacteria)	K06415	spoVR; stage V sporulation protein R
	Sporulation (Actinobacteria)	K06416	spoVS; stage V sporulation protein S
	Sporulation (Actinobacteria)	K06417	spoVID; stage VI sporulation protein D
	Sporulation (Actinobacteria)	K06437	yknT; sigma-E barrenled sporulation protein
	Sporulation (Actinobacteria)	K06438	yqfD; similar to stage IV sporulation protein
	Sporulation (Actinobacteria)	K07697	kinB; two-component system, sporulation sensor kinase B [EC:2.7.13.3]
	Sporulation (Actinobacteria)	K07698	kinC; two-component system, sporulation sensor kinase C [EC:2.7.13.3]
	Sporulation (Actinobacteria)	K07699	spo0A; two-component system, response regulator, stage 0 sporulation protein A
	Sporulation (Actinobacteria)	K08293	SMK1; sporulation-specific mitogen-activated protein kinase SMK1 [EC:2.7.11.24]
	Sporulation (Actinobacteria)	K08384	spoVD; stage V sporulation protein D (sporulation-specific penicillin-binding protein)
	Glycogen synthesis	K08822	GSK3A; glycogen synthase kinase 3 alpha [EC:2.7.11.26]
	Sporulation (Actinobacteria)	K12576	SPO12; sporulation-specific protein 12
	Sporulation (Actinobacteria)	K12771	SPS1; sporulation-specific protein 1 [EC:2.7.11.1]
	Sporulation (Actinobacteria)	K12772	SPS4; sporulation-specific protein 4
	Sporulation (Actinobacteria)	K12773	SPR3; sporulation-regulated protein 3
	Sporulation (Actinobacteria)	K12783	SSP1; sporulation-specific protein 1
	Sporulation (Actinobacteria)	K13532	kinD; two-component system, sporulation sensor kinase D [EC:2.7.13.3]
	Sporulation (Actinobacteria)	K13533	kinE; two-component system, sporulation sensor kinase E [EC:2.7.13.3]
	Glycogen synthesis	K16150	K16150; glycogen synthase [EC:2.4.1.11]
	Exopolysaccharide synthesis	K16566	exoY ; exopolysaccharide production protein ExoY
	Exopolysaccharide synthesis	K16567	exoQ ; exopolysaccharide production protein ExoQ
	Exopolysaccharide synthesis	K16568	exoZ ; exopolysaccharide production protein ExoZ
	Sporulation (Actinobacteria)	K16947	SPR28; sporulation-regulated protein 28
	Glycogen synthesis	K20812	glgA; glycogen synthase [EC:2.4.1.242]

https://doi.org/10.5194/soil-2021-88
Preprint. Discussion started: 1 September 2021

Table A4. Chlorophyll concentrations and water content values in the biocrust at each sampling point and site.

Time	Chlorophyll concentration (mg chla/ g soil)	Water content (%)	Total organic carbon (%)	Total nitrogen (%)	Polysaccharides
T[0]	7.7	1.9	4.2	0.1	63.6
T[0]	8.6	2.7	4.1	0.1	69.4
T[0]	6.8	2.3	4.2	0.1	64.2
T[R]	10.1	13.6	3.0	0.1	54.3
T[R]	16.1	16.9	3.9	0.1	224.5
T[R]	15.7	16.6	3.8	0.1	134.8
T[R]	12.7	16.3	4.0	0.1	111.4
T[R]	14.2	17.5	4.0	0.1	157.1
T[1]	10.5	5.3	3.3	0.1	121.6
T[1]	16.0	5.6	3.2	0.1	82.6
T[1]	16.9	7.1	4.0	0.1	145.5
T[1]	15.3	6.2	4.0	0.1	168.9
T[1]	14.2	6.8	3.9	0.1	199.6
T[2]	10.1	3.9	3.9	0.1	78.4
T[2]	11.8	4.5	4.0	0.1	85.0
T[2]	11.8	4.5	4.2	0.1	133.3
T[2]	13.0	5.1	4.1	0.1	111.0
T[2]	13.0	6.9	4.1	0.1	59.8
T[3]	9.9	2.9	3.8	0.1	66.7
T[3]	12.8	3.7	3.7	0.1	78.4
T[3]	9.3	3.7	3.7	0.1	39.9
T[3]	9.4	4.3	4.5	0.1	75.7
T[3]	14.5	3.8	4.6	0.1	102.2

https://doi.org/10.5194/soil-2021-88
Preprint. Discussion started: 1 September 2021

Table A5. Dunn tests p values for chlorophyll concentration (mg chla/g of soil), water content (%), total organic carbon content (%) and total nitrogen (%) in biocrust samples collected at the different sampling point. Bold numbers mark significant differences (<0.05).

Comparison	Chlorophyll	Water content	Total organic Carbon	Total Nitrogen	Polysaccharides
T[0] - T[1]	**5.4E-03**	5.7E-02	8.9E-01	1.7E-01	**4.60E-02**
T[0] - T[2]	**2.8E-02**	3.6E-01	6.4E-01	5.3E-01	7.34E-01
T[1] - T[2]	2.6E-01	**2.6E-02**	5.5E-01	4.5E-01	9.00E-02
T[0] - T[3]	1.8E-01	2.0E-01	7.5E-01	6.5E-02	6.93E-01
T[1] - T[3]	5.3E-02	**8.0E-03**	8.5E-01	6.1E-01	**2.00E-02**
T[2] - T[3]	1.7E-01	3.2E-01	4.3E-01	2.1E-01	4.64E-01
T[0] - T[R]	**3.6E-06**	1.6E-01	8.4E-01	7.2E-01	2.04E-01
T[1] - T[R]	**2.6E-02**	2.8E-01	9.5E-01	3.0E-01	4.26E-01
T[2] - T[R]	**4.9E-03**	8.6E-02	5.1E-01	7.8E-01	3.45E-01
T[3] - T[R]	**1.9E-04**	**3.3E-02**	9.0E-01	1.3E-01	1.02E-01

https://doi.org/10.5194/soil-2021-88
Preprint. Discussion started: 1 September 2021

Table A6. Relative abundance of the taxa in the biocrust community at each time point.

Phylum	Order	Time Point	Relative Abundance
Actinobacteria	Frankiales	T[0]	0.023
		T[R]	0.036
		T[1]	0.013
		T[2]	0.032
		T[3]	0.021
	IMCC26256	T[0]	0.0097
		T[R]	0.0053
		T[1]	0.0084
		T[2]	0.0086
		T[3]	0.0062
	Micrococcales	T[0]	0.39
		T[R]	0.0098
		T[2]	0.0082
		T[3]	0.0067
	Micromonosporales	T[R]	0.014
		T[1]	0.0056
		T[2]	0.0075
		T[3]	0.0075
	Microtrichales	T[1]	0.0053
		T[2]	0.0054
	Propionibacteriales	T[R]	0.011
		T[1]	0.0062
		T[2]	0.0095
		T[3]	0.0053
	Pseudonocardiales	T[R]	0.0079
		T[2]	0.0054
	Rubrobacterales	T[0]	0.015
		T[R]	0.075
		T[1]	0.088
		T[2]	0.1
		T[3]	0.08
	Solirubrobacterales	T[0]	0.077
		T[R]	0.04
		T[1]	0.043
		T[2]	0.046
		T[3]	0.032
Cyanobacteria	Chloroplast	T[0]	0.021
		T[R]	0.012
		T[1]	0.027
		T[2]	0.028
		T[3]	0.018
	Cyanobacteriales	T[0]	0.19
Cyanobacteria	Cyanobacteriales	T[R]	0.39
		T[1]	0.33

https://doi.org/10.5194/soil-2021-88
Preprint. Discussion started: 1 September 2021

		T[2]	0.29
		T[3]	0.35
	Unknown Oxyphotobacteria	T[R]	0.013
		T[1]	0.015
		T[2]	0.014
		T[3]	0.015
	Thermosynechococcales	T[0]	0.011
Acidobacteriota	Bryobacterales	T[R]	0.0052
Bacteroidota	Chitinophagales	T[0]	0.0062
		T[R]	0.0052
		T[2]	0.0073
	Cytophagales	T[0]	0.0092
		T[R]	0.096
		T[1]	0.12
		T[2]	0.079
		T[3]	0.091
Chloroflexi	Kallotenuales	T[R]	0.0084
		T[2]	0.016
		T[3]	0.0084
	Thermomicrobiales	T[2]	0.0051
Gemmatimonadota	Gemmatimonadales	T[R]	0.0054
		T[2]	0.0069
	Longimicrobiales	T[R]	0.016
		T[2]	0.0054
Myxococcota	Haliangiales	T[R]	0.0057
		T[3]	0.006
	Myxococcales	T[R]	0.02
		T[1]	0.011
		T[2]	0.014
		T[3]	0.015
	Nannocystales	T[R]	0.0088
		T[1]	0.011
		T[2]	0.0056
		T[3]	0.0067
	Polyangiales	T[R]	0.0083
		T[1]	0.0081
		T[2]	0.006
		T[3]	0.0066
Proteobacteria	Acetobacterales	T[R]	0.015
		T[1]	0.012
		T[2]	0.016
		T[3]	0.016
	Azospirillales	T[0]	0.031
	Burkholderiales	T[0]	0.057
Proteobacteria	Burkholderiales	T[R]	0.013
		T[1]	0.011

https://doi.org/10.5194/soil-2021-88
Preprint. Discussion started: 1 September 2021

		T[2]	0.014
		T[3]	0.013
	Caulobacterales	T[0]	0.013
		T[R]	0.022
		T[1]	0.035
		T[2]	0.021
		T[3]	0.025
	Pseudomonadales	T[0]	0.014
	Rhizobiales	T[0]	0.087
		T[R]	0.044
		T[1]	0.063
		T[2]	0.07
		T[3]	0.068
	Rhodobacterales	T[0]	0.0055
		T[R]	0.016
		T[1]	0.017
		T[2]	0.021
		T[3]	0.016
	Sphingomonadales	T[0]	0.019
		T[R]	0.038
		T[1]	0.044
		T[2]	0.044
		T[3]	0.034
Verrucomicrobiota	Chthoniobacterales	T[R]	0.012
		T[1]	0.067
		T[2]	0.044
		T[3]	0.095

https://doi.org/10.5194/soil-2021-88
Preprint. Discussion started: 1 September 2021

Table A7. P-values of the Dunn tests between time points on the relative abundance of the actinobacterial and cyanobacterial orders. Bold numbers are significant (<0.05).

Comparison	Cyanobacteria	Actinobacteria
T[0] - T[1]	**6.1E-10**	**8.2E-13**
T[0] - T[2]	**5.1E-08**	**2.5E-14**
T[0] - T[3]	**6.0E-10**	**6.9E-11**
T[0] - T[R]	**6.5E-10**	**6.5E-14**
T[1] - T[3]	5.0E-01	2.3E-01
T[1] - T[2]	1.9E-01	2.9E-01
T[1] - T[R]	5.0E-01	3.5E-01
T[2] - T[R]	1.9E-01	4.4E-01
T[3] - T[R]	4.9E-01	1.3E-01
T[2] - T[3]	1.9E-01	9.9E-02

https://doi.org/10.5194/soil-2021-88
Preprint. Discussion started: 1 September 2021

Table A8. Abundance (in copy number (CN)) of each time points within each group of gene.

Gene Group	Time points	Abundance
DNA conservation	T[0]	20590
	T[R]	91433
	T[1]	92496
	T[2]	78321
	T[3]	81983
DNA repair and degradation	T[0]	13579
	T[R]	66132
	T[1]	67048
	T[2]	55948
	T[3]	58457
Light energy or sensing	T[0]	85
	T[R]	43
	T[1]	59
	T[2]	64
	T[3]	17
Lithotrophs	T[0]	7554
	T[R]	37972
	T[1]	38632
	T[2]	31341
	T[3]	32758
Nitrogen	T[0]	10027
	T[R]	50708
	T[1]	58068
	T[2]	48225
	T[3]	45638
Organotrophs	T[0]	60007
	T[R]	108275
	T[1]	111044
	T[2]	88557
	T[3]	89148
Phototrophy	T[0]	50301
	T[R]	445432
	T[1]	425819
	T[2]	342188
	T[3]	407532
ROS-damage prevention	T[0]	26126
	T[R]	138367
	T[1]	143726
	T[2]	121507
	T[3]	126677
Sensing & motility	T[0]	31075
	T[R]	81947
	T[1]	92070
Sensing & motility	T[2]	90844

https://doi.org/10.5194/soil-2021-88
Preprint. Discussion started: 1 September 2021

	T[3]	74436
Sporulation capsule & C-storage	T[0]	7302
	T[R]	48141
	T[1]	48944
	T[2]	38998
	T[3]	42341

https://doi.org/10.5194/soil-2021-88
Preprint. Discussion started: 1 September 2021

Table A9. Chi-square values and p-values of the Dunn tests between time points done on the functional prediction results. Bold numbers are significant (< 0.05)

Comparison	DNA Conservation	DNA Repair	Light energy	Lithotrophy	Nitrogen
T[0] - T[1]	**4.9E-03**	**2.9E-03**	1.9E-01	**3.1E-04**	**4.2E-17**
T[0] - T[2]	**2.0E-02**	**9.7E-03**	4.5E-01	**7.5E-03**	**8.1E-12**
T[0] - T[3]	**2.9E-02**	**1.6E-02**	2.8E-01	**1.5E-02**	**8.2E-10**
T[0] - T[R]	**2.9E-02**	**5.2E-03**	3.8E-01	**1.6E-03**	**1.3E-12**
T[1] - T[3]	2.1E-01	2.4E-01	**4.6E-02**	7.3E-02	**4.0E-03**
T[1] - T[2]	2.7E-01	3.1E-01	2.0E-01	1.3E-01	**3.3E-02**
T[1] - T[R]	2.2E-01	4.1E-01	2.6E-01	2.9E-01	6.3E-02
T[2] - T[3]	4.3E-01	4.2E-01	2.0E-01	3.8E-01	2.1E-01
T[2] - T[R]	4.3E-01	4.0E-01	4.2E-01	2.8E-01	3.8E-01
T[3] - T[R]	5.0E-01	3.2E-01	1.5E-01	1.8E-01	1.3E-01
Chi-square	7.0E+00	8.9E+00	2.9E+00	1.3E+01	7.6E+01

Comparisons	Organotrophy	Phototrophy	ROS	Motility	Sporulation
T[0] - T[1]	**1.9E-03**	**5.4E-36**	**5.7E-06**	**1.1E-18**	**7.5E-05**
T[0] - T[2]	**2.1E-02**	**8.5E-17**	**2.8E-05**	**2.1E-14**	**3.0E-09**
T[0] - T[3]	**4.1E-02**	**8.8E-26**	**9.0E-05**	**2.4E-11**	**8.8E-04**
T[0] - T[R]	**1.9E-02**	**4.3E-35**	**6.3E-05**	**1.2E-14**	**4.1E-04**
T[1] - T[3]	9.1E-02	**9.3E-03**	2.3E-01	**6.1E-03**	2.2E-01
T[1] - T[2]	1.6E-01	**5.2E-07**	3.4E-01	8.4E-02	**9.7E-03**
T[1] - T[R]	1.7E-01	4.2E-01	2.6E-01	9.7E-02	3.0E-01
T[2] - T[3]	3.7E-01	**5.7E-03**	3.7E-01	1.3E-01	**9.5E-04**
T[2] - T[R]	4.8E-01	**1.4E-06**	4.1E-01	4.7E-01	**2.2E-03**
T[3] - T[R]	3.5E-01	**1.5E-02**	4.6E-01	1.1E-01	4.0E-01
Chi-square	8.6E+00	2.0E+02	2.3E+01	8.7E+01	3.5E+01

https://doi.org/10.5194/soil-2021-88
Preprint. Discussion started: 1 September 2021

APPPENDIX B

Figures

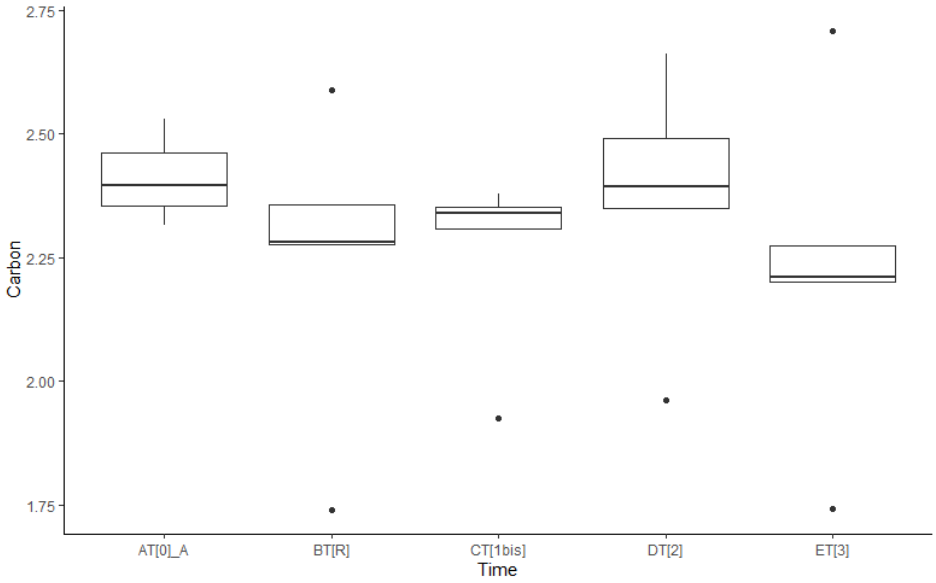

Figure B1. Boxplot of the organic carbon content (%) for each sampling point.

https://doi.org/10.5194/soil-2021-88
Preprint. Discussion started: 1 September 2021

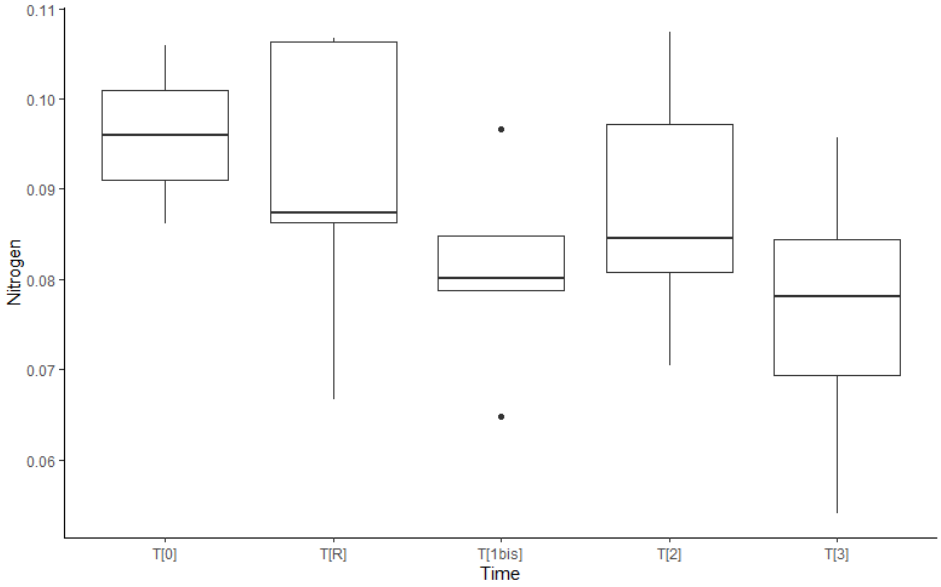

Figure B2. Boxplot of the nitrogen content (%) for each time point.